


Spring 2019

Increased Utility of pH Sensitive Indicators as High Concentration CO₂ Detectors Through the Use of Polyelectrolyte Complexes as Stabilizing Media

Camden James Johnson
Central Washington University, cjohnson1325@gmail.com

Follow this and additional works at: <https://digitalcommons.cwu.edu/etd>

 Part of the [Analytical Chemistry Commons](#), [Inorganic Chemistry Commons](#), [Materials Chemistry Commons](#), and the [Polymer Chemistry Commons](#)

Recommended Citation

Johnson, Camden James, "Increased Utility of pH Sensitive Indicators as High Concentration CO₂ Detectors Through the Use of Polyelectrolyte Complexes as Stabilizing Media" (2019). *All Master's Theses*. 1195.

<https://digitalcommons.cwu.edu/etd/1195>

This Thesis is brought to you for free and open access by the Master's Theses at ScholarWorks@CWU. It has been accepted for inclusion in All Master's Theses by an authorized administrator of ScholarWorks@CWU. For more information, please contact scholarworks@cwu.edu.

Increased Utility of pH Sensitive Indicators as High Concentration CO₂ Detectors Through the
Use of Polyelectrolyte Complexes as Stabilizing Media

A Thesis

Presented to

The Graduate Faculty

Central Washington University

In Partial Fulfillment

of the Requirements for the Degree

Master of Science

Chemistry

by

Camden James Johnson

May 2019

CENTRAL WASHINGTON UNIVERSITY

Graduate Studies

We hereby approve the thesis of

Camden James Johnson

Candidate for the degree of Master of Science

APPROVED FOR THE GRADUATE FACULTY

Dr. Dion Rivera, Committee Chair

Dr. JoAnn Peters

Dr. Yingbin Ge

Dean of Graduate Studies

ABSTRACT

Increased Utility of pH Sensitive Indicators as High Concentration CO₂ Detectors Through the Use of Polyelectrolyte Complexes as Stabilizing Media

By

Camden James Johnson

May 2019

Development of plastic materials which produce visible color change when exposed to different environments has recently attracted attention for many biomedical applications.^{1,2} Many biomedical devices are packaged under high concentrations of carbon dioxide (CO₂) which can lower the pH of the packaging environment. This is similar to the CO₂ chemistry responsible for ocean acidification.³ Dye molecules that are sensitive to environmental changes in pH (known as pH indicators) can be encapsulated in plastics and produce a visible color change when a medical device is removed from the sterile CO₂ environment. Plastics made from large molecules known as polyelectrolytes can form complexes which may serve as inexpensive and multipurpose mediums for encapsulation of pH sensitive indicators. This research aims to combine the properties of both pH indicators and polyelectrolyte complexes (PECs) to form a stable plastic which will contain indicators sensitive to CO₂ environments and slowly change color over extended periods of time, increasing the durability and usefulness in many such biomedical applications. Characterization of the physical properties of indicator containing polyelectrolyte complexes (ICPECs) was performed via scanning electron microscopy (SEM) in order to determine properties such as pore size. Compositional analysis of the ICPEC was performed via

attenuated total reflection infrared spectroscopy (ATR-FTIR) and simultaneous thermal analysis (STA). It was shown that ICPECs are very dependent on both internal ionic concentration and moisture content and that these factors can significantly influence the rate at which ICPECs respond to introduction to high concentration CO₂ environments such as are found in many biomedical applications.

ACKNOWLEDGEMENTS

I would like to express my gratitude to my advisor, Dr. Dion Rivera, as well as my committee members Dr. JoAnn Peters and Dr. Yingbin Ge. I would also like to thank Central Washington University School of Graduate Studies and Research for the 2017 Master's Student Research & Creative Activities Fellowship.

TABLE OF CONTENTS

Chapter	Page
I. INTRODUCTION	1
Packing Techniques	1
Medical Device Packaging	2
pH Sensitive CO ₂ Monitoring Systems	3
Previous MAP Monitoring Devices.....	3
Introduction to Polyelectrolyte Complexes	7
Polyelectrolyte Stabilization of Charged Species	10
Thesis Research	11
II. METHODS	13
Materials	13
Preparation of PECs	13
Preparation of ICPECs	15
ICPEC Variants.....	18
Analysis of Internal Moisture Content.....	18
Time Lapse Photography	20
Analysis of Morphology	21
ICPEC Analysis of Polyelectrolyte Concentration	23
III. RESULTS AND DISCUSSION	26
Analysis of Internal Moisture and Moisture Uptake.....	26
Time Lapse Studies	33
Morphological Studies	49
Analysis of Polyelectrolyte Concentration	55
IV. CONCLUSIONS.....	63
V. REFERENCES	67

LIST OF TABLES

<u>Table</u>	<u>Page</u>
2.1 A general dilution scheme of buffer gradient samples for preparation of ICPECs	16
2.2 An example of the salt gradient within the ICPEC reaction mixture using NaCl	17
3.1 Internal moisture content via % mass loss of standard ICPECs. Note that the elapsed time listed was after the initial 24 drying process. Note the first 17 samples listed are ICPECS prepared with the standard method, and the last 3 samples are PECs prepared with the standard method.	28
3.2 Internal moisture content of the ICPECs after being subjected to an atmosphere with a constant relative humidity for a 48 hour equilibration period. LiCl, K ₂ CO ₃ , and NaCl generate atmospheres with relative humidities of 11%, 43%, and 75% respectively. Note all elapsed times before sampling are after the 24 hour initial drying period and the 48 hour atmospheric subjection period.	30
3.3 Various samples and their listed time responses to CO ₂ exposure. Samples ID's are roughly indicative of chronological order. All listed samples utilized the phenol red indicator within the ICPEC. % Humidity refers to the humidity of the atmosphere which the samples were exposed after drying.	34
3.4 Phenol red ICPECs sample sets designed to compared drying temperature and time response.....	38
3.5 Percent mass loss gathered via STA and absorbance of water stretching modes in the IR spectrum.....	42
3.6 Phenol red ICPECs sample sets designed to compare counterion concentration in complex mixture and time response.	43

3.7	Phenol red ICPECs sample sets designed to compare increased buffer addition in complex mixture and time response.	46
3.8	Time responses of various phenol red ICPECs as a function of the controlled humidity to which each sample was exposed to prior to time lapse photography.	48
3.9	Samples which utilized m-cresol purple as the pH sensitive indicator and the response times of those samples.	49
3.10	Two standard PECs and the resulting concentrations of polycation and polyanion remaining in the supernatant solutions after precipitation of the PEC.	61
3.11	Calculated values for K_{eq} and ΔG°_{rxn} of standard PECs assuming 20 °C as the laboratory temperature.	61
3.12	Concentrations and resulting mol ratios of the polyelectrolytes present in the supernatant solution after formation of the ICPEC made using the standard preparation method.	62
3.13	Calculated values for K_{eq} and ΔG°_{rxn} of standard ICPECs assuming 20 °C as the laboratory temperature.	62

LIST OF FIGURES

<u>Figure</u>	<u>Page</u>
1.1 Equilibrium of CO ₂ and H ₂ CO ₃ during first deprotonation (Top). Reaction between H ₂ CO ₃ and Phenol Red (Middle). Deprotonated and protonated forms of the pH sensitive indicator phenol red (Bottom).....	3
1.2 Both oxidized and reduced forms of ITS	4
1.3 Graphic representation of thin-films developed by Heacock et. al. ¹⁴	5
1.4 Monomer units for poly(diallyldimethylammonium) on left and poly(styrene 4-sulfonate) on right. Both are shown without the respective counterions in order to illustrate areas of charge.	8
1.5 A depiction of the formation of PECs within the solution phase.	8
1.6 A PEC made using the standard method. Following precipitation, the PEC solid was pressed into a 1 mm deep, 3cm wide washer and allowed to air dry for 24 hours.	8
1.7 On left a monomer unit of PDADMA with the Cl counterion which forms the polyelectrolyte encapsulation of ITS in the leuco form on right.	10
1.8 Concentration of anionic phenol red against the interface of the PDADMA cationic polyelectrolyte along with the anionic hydroxide species.	11
2.1 Structures of benzethonium chloride (left) and cetylpyridinium chloride (right).....	18
2.2 Visual transition of phenol red ICPEC within a high CO ₂ atmosphere in an eight-hour timeframe.	21

3.1	STA data showing decreasing mass (green) of the sampled ICPEC as a function of temperature (red) and time. Notice the DSC curve (blue) which was used to establish direct heating endpoints.	27
3.2	Convergence of internal moisture content within ICPECs to atmospheric humidity ~15%. Note the elapsed times listed are in addition to the initial 24 hour drying period.	29
3.3	Relationship between internal water content of sample and the relative humidity of the atmosphere in which the sample was placed. Note the point (red) which corresponds to proper preparation of the K_2CO_3 saturated solution.	31
3.4	Corrected correlation between internal moisture content of the ICPEC and the relative humidity of the atmosphere in which the ICPEC was equilibrated.	33
3.5	Net neutral charge maintenance by both extrinsic charge coupling (left and right boxes) and intrinsic charge coupling (middle box). ¹⁷	37
3.6	A visualization of the density gradient present within a PEC as counterions are added to the complex mixture where anions and polyanions are shown in red and cations and polycations are shown in blue. (counterion concentration increases from left to right). ¹⁹	37
3.7	Two phenol red ICPECs where one is air dried (left) and the other is dried at 70 °C for 1 hour before being air dried (right).	38
3.8	Absorbance data gathered via ATR-FTIR over three days of the ICPEC sample 66P examining the increase in the absorbance associated with water stretching modes as a function of time.	42
3.9	Three phenol red ICPECs prepared from counterion solutions with concentrations 250 mM (left), 50 mM (center), and 0 mM for control (right)	43

3.10	Three of five phenol red samples in the 94P sample set showing 1x buffer composition (left), 2x buffer composition (center), and 4x buffer composition (right). ICPECs with 1/2x and 1/4x buffer concentrations formed thin films which weren't able to be photographed in whole samples due to fragile composition. Note the increase in the reflective surface of the ICPECs from left to right.	46
3.11	Two phenol red ICPECs having been exposed to atmospheres with controlled humidities for 48 hours. The ICPEC which was exposed to a 75% relative humidity (left) appears much more translucent and brighter in color than the ICPEC dried in a 11% relative humidity (right).....	48
3.12	One m-cresol purple ICPEC shown before (left) and after (right) exposure to a high CO ₂ environment for 50 hours.....	49
3.13	Images of the rough (left) and smooth (right) regions on a PEC under SEM at 80x magnification	51
3.14	SEM images of the PEC rough structure at 600, 2500, 5000, and 20000x magnification.	52
3.15	SEM images of the PEC smooth structure at 600, 2500, 5000, and 20000x magnification.	53
3.16	SEM images of PECs made under standard conditions (top left), with 50 mM NaCl (top right), and 250 mM NaCl (bottom).....	55
3.17	SEM images of PECs made under standard conditions (top left), with 50 mM NaCl (top right), and 250 mM NaCl (bottom) with an apparent trend of decreasing porosity as a function of counterion concentration	56
3.18	Linear calibration curve for PSSNa at 224 nm	57

- 3.19 Standard calibration curve for PDADMAC at 590 nm. The bracketed region represents the approximate utilized region from 4.48×10^{-7} to 9.87×10^{-6} 58
- 3.20 Stacked spectrum of the absorbance of PDADMAC as a function of increased concentration. Note the shift of the max absorbing wavelength on the peak ~ 590 nm... 59

LIST OF ABBREVIATIONS

Abbreviation	Explanation
ABS	Acrylonitrile butadiene styrene
ATR-FTIR	Attenuated total reflectance- Fourier transform infrared spectroscopy
CO ₂	Carbon dioxide
DSC	Differential scanning calorimetry
H ₂ CO ₃	Carbonic acid
ICPEC	Indicator containing polyelectrolyte complex
ITS	Indigo tetrasulfonate
K ₂ CO ₃	Potassium carbonate
LiCl	Lithium Chloride
MAP	Modified atmosphere packaging
NaCl	Sodium Chloride
PDADMAC	Poly(diallyldimethylammonium chloride)
PEC	Polyelectrolyte complex
PEM	Polyelectrolyte multilayer
PSSNa	Poly(sodium 4- styrenesulfonate)
SEM	Scanning electron microscopy
STA	Simultaneous thermal analysis
TGA	Thermogravimetric analysis

1. INTRODUCTION

I. Packaging Techniques

Large scale industrial applications of packaging which utilizes modified atmospheric packaging (MAP) techniques to inhibit the growth of bacteria and other microorganisms leading to food spoilage or potential health risks has been commonplace since the late 1980's.⁴⁻⁶ Usage of specifically CO₂ gas within these MAP techniques has shown great utility within the food, and more recently, the medical industries due to the ability for high CO₂ concentration atmospheres to not only inhibit bacterial growth but to also significantly diminish microbial populations. Inhibition of microorganism growth is largely due to the decrease of environmental pH that is a result of the equilibrium shift which occurs in high CO₂ gas concentrations, forming carbonic acid (H₂CO₃) on the surface of the product contained within the MAP system.^{3,4} When the packaging system is compromised via either opening of the package or failure of the packaging system, the CO₂ is released rapidly from the system. Equilibrium shifts to the formation of CO₂ gas from carbonic acid, readying the enclosed product for use without incurred complication from the sterilization technique used for packaging. Such issues as may be encountered when sterilization techniques such as preservatives are utilized to this end. Recently this approach has been utilized within many medical industries across the world in order to maintain sterile environments within medical device packaging, as packing under CO₂ can be accomplished cheaply, rapidly, and without concern for contamination of procedures during end-use.

Microbial growth inhibition sufficient for medical device packaging requires CO₂ concentrations within a packaging system upwards of 70% CO₂.^{5,7} Though the permeability of CO₂ through many modern flexible plastics can be selected to be relatively low, there still remains a significant need for a CO₂ monitoring system to be present within sensitive medical

device packaging to determine that the device is maintaining atmospheric CO₂ levels which ensure the sterility of the enclosed device.⁸

II. Medical Device Packaging

Medical device packaging, like other MAP techniques, utilizes high internal CO₂ concentrations in order to inhibit microbial growth and preserve sterility.⁷ This practice is used commonly in most modern medical industries throughout the world. Unlike other MAP techniques, medical device packaging utilizes near 100% internal CO₂ concentrations as the internal components can suffer no damage from decreased environmental pH.⁴⁻⁷ High concentration CO₂ environments also ensure microbial growth will be sufficiently inhibited over extended periods of time as many medical devices can be stored for upwards of 12 months which is considerably longer than most other MAP systems.

Also required is the ability of the medical device and its packaging to endure those processes which are needed for complete sterilization where sterility is defined as “having not more than one viable microorganism in a million sterilized products”.⁷ These processes include gamma irradiation, ethylene oxide sterilization, heat sterilization, and gas plasma sterilization. Most commonly a packaging system will endure at minimum gamma irradiation sterilization as it is the most cost-effective of the sterilization techniques. If a packaging system cannot endure gamma irradiation, another technique or a mixture of techniques will be utilized for sterilization which will not degrade the device or packaging system. As packing under high concentrations of CO₂ is a method by which to ensure the sterility of a device within an enclosed packaging system, it is desirable for the internal CO₂ of a packaging system to be monitored.

III. pH Sensitive CO₂ Monitoring Systems

Many current technologies for measuring environmental CO₂ concentrations utilize pH sensitive indicators such as phenolsulfonphthalein (phenol red) in order to achieve clear visual indication of the current environmental CO₂ concentration. This is due to the fact that environments containing high concentrations of CO₂ favor the formation of H₂CO₃ when moisture is present, decreasing environmental pH, and protonating the encapsulated indicator. The protonated form of the phenol red is visible as a yellow color where the de-protonated form is pink, resulting in a clear color change as a function of environmental pH as is seen in Figure 1.1.¹

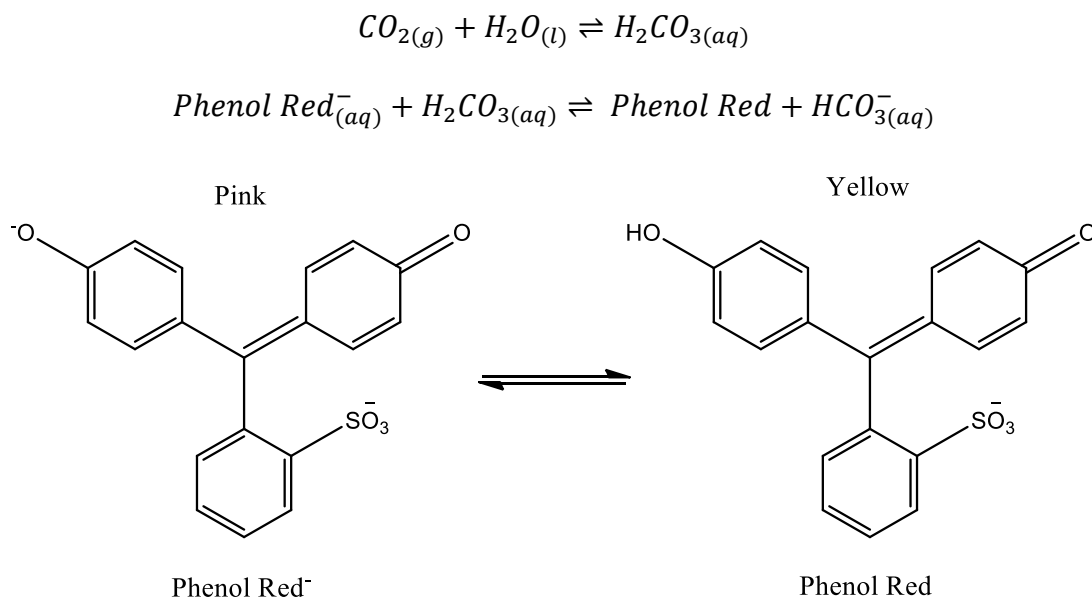


Figure 1.1 Equilibrium of CO₂ and H₂CO₃ during first deprotonation (Top). Reaction between H₂CO₃ and Phenol Red (Middle). Deprotonated and protonated forms of the pH sensitive indicator phenol red (Bottom).

IV. Previous MAP Monitoring Devices

Devices which utilize pH sensitive indicators to provide clear indication of product quality to the end user have been produced in many variants. Limitation on aerobic microbial growth is of

the primary modern methods of MAP preservation of food products.⁶ Many such technologies utilize the presence of oxygen in order to determine package failure or expiration within MAP processes which limit or remove oxygen from the packaging environment. One such device developed by Mills et al. utilizes the redox sensitive dye indigo-tetrasulfonate (ITS) encapsulated within hydroxyethyl cellulose based plastic films.⁹ ITS is deep blue while in the oxidized form and upon addition of a strong reductant is reduced to leuco-ITS which exhibits a pale yellow color as seen in Figure 1.2. While in solution phase the ITS is exposed to a reducing agent and is then mixed into a semi-plastic suspension. Spun at 2500 rpm this suspension becomes a thin film and is then stored in a dark oxygen free environment until use. Presence of oxygen within the sensor environment at atmospheric concentrations (21%) or higher induces immediate irreversible color change from leuco-ITS to the oxidized ITS species.

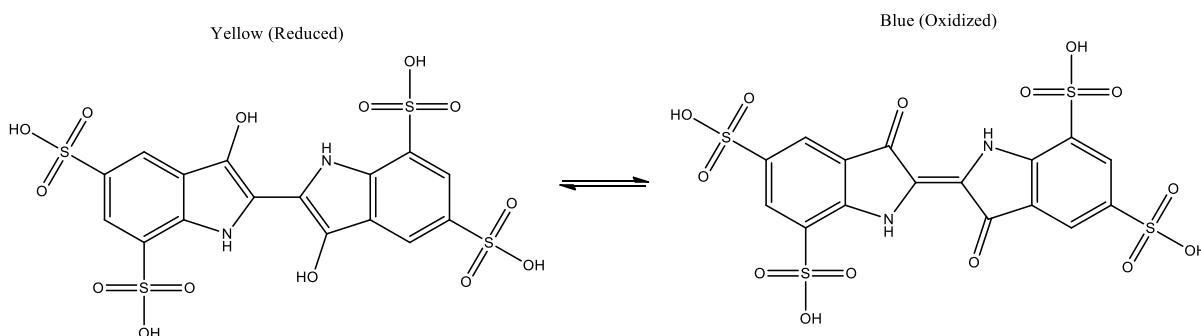


Figure 1.2 Both oxidized and reduced forms of ITS

Advantageous to these devices was the use of an indicator in which both the oxidized and reduced forms were visible without the use of instrumentation. Previous technologies utilizing redox sensitive indicators often relied on expensive external instrumentation in order to visualize indicator changes within the UV or near UV spectrum, which significantly limited practical application.^{10,11} Preparation of species which readily react with atmospheric concentrations of

oxygen however is time consuming involving multiple freeze-thaw processes and non-conventional storage. While these devices showed remarkable stability under anerobic conditions, photobleaching and irreversible color change occurred in aerobic conditions.^{9,12}

More recently, plastic thin-films have been developed in order to meet the need for high-concentration CO₂ monitoring devices, which can fit within packaging around medical devices. Devices created by Heacock et al. based on a design from Mills et al. utilize a three layer plastic system in order to create a CO₂ monitor which is sensitive to removal from high CO₂ concentration environments (Figure 1.3).^{1,2,13,14} Advantageous to this system is the shift from aqueous CO₂ detection systems which show limited use in many packaging systems. The lowermost of these three layers serves as a flexible substrate to which the device can be affixed to a medical device. Indicator sensitive to change in pH is mixed within the plastic of the second layer, which is then saturated with CO₂. When the device is removed from an all CO₂ environment, equilibrium within the saturated CO₂ layer immediately shifts to the formation of CO₂ which begins to leave the saturated layer. The uppermost layer serves as a diffusion layer by which the rate at which CO₂ escapes from the first layer is limited.

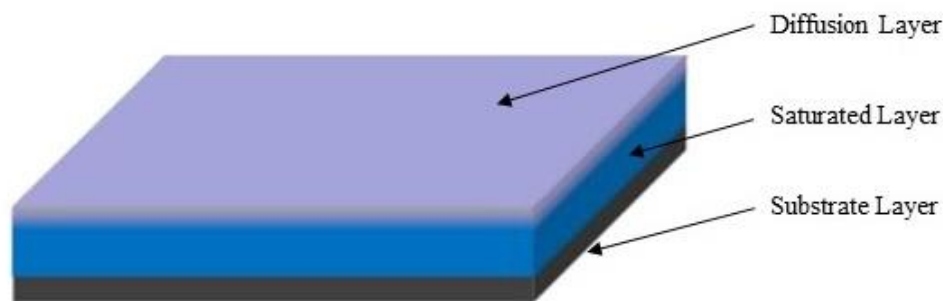


Figure 1.3 Graphic representation of thin-films developed by Heacock et. al.¹⁴

Limitation of the rate at which diffusion of CO₂ from the saturated layer occurs allows for the device to be removed from a high concentration CO₂ environment temporarily without compromising the device. Evacuation of CO₂ from the saturated layer without this rate limiting diffusion layer would occur rapidly. Diffusion of CO₂ through the diffusion layer is effectively one-way, meaning complete evacuation of CO₂ from the saturated layer would render the device depleted. Heacock et al. also multi-purposed this diffusion layer by determining the thickness dependent rate at which CO₂ diffusion was limited. Specific time responses of the thin-film device were then developed to allow for further utility of the device.^{1,2,14}

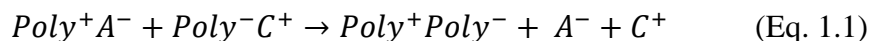
Increased utility of the CO₂ monitoring system via a tunable predetermined time response developed by Heacock et al. was sought through the potential lessening of bookkeeping by staff members within medical facilities.¹⁴ Patients with need for intravenous devices within most medical facilities must have those devices changed or replaced every 24 to 96 hours depending on the device and whether or not it contains particular medications.¹⁵ A CO₂ monitor affixed to a medical device which has a time response tuned to that which is required of the specific medical device might eliminate the need for recordkeeping or exchange rotations. Need for regular replacement can lead to unneeded trauma to a patient.¹⁵ Use of pH sensitive indicators with time responsive diffusion layers allows for medical device sanitation evaluations to be made rapidly.

These devices are limited in use however due to the complexity and cost of production, as well as the physical conditions which they can withstand. As modern medical devices need to be subjected to high heat cycling, gamma irradiation, and other sterilization techniques, all equipment contained within the packaging must be able to withstand these extreme conditions.⁷

To address the need for a more robust and cost-effective CO₂ monitoring system, research has been conducted by this group on the use of ICPECs which might function more effectively in those environments required of medical devices and medical device packaging systems.

V. Introduction to Polyelectrolyte Complexes

Polymers are formed from long repeating chains of smaller monomer units. Polymers which possess a net electrical charge are known as polyelectrolytes. Strong polyelectrolytes are polymers in which every monomer unit within the polyelectrolyte possess a net electrostatic charge. Polyelectrolyte complexes form when polyelectrolytes of opposing charge are brought together in the solution phase, and form a net neutral complex as is described in Equation 1.1.¹⁶ The mechanism of this complexation has been traditionally described via Coulombic attraction between the positively charged polyelectrolyte (polycation) and the negatively charged polyelectrolyte (polyanion) when liberated from their respective counterions while in solution. However, recent work performed within this group, as well as externally, suggests there also exists a significant entropic driving force for this polyelectrolyte complexation.¹⁷⁻¹⁹ An example of the most frequently used polycation and polyanion in this research, poly(diallyldimethylammonium chloride) (PDADMAC) and poly(sodium 4-styrenesulfonate sodium) (PSSNa) are seen in Figure 1.4. A depiction of the complexation process is given in Figure 1.5 which yields a product such as is seen in Figure 1.6.



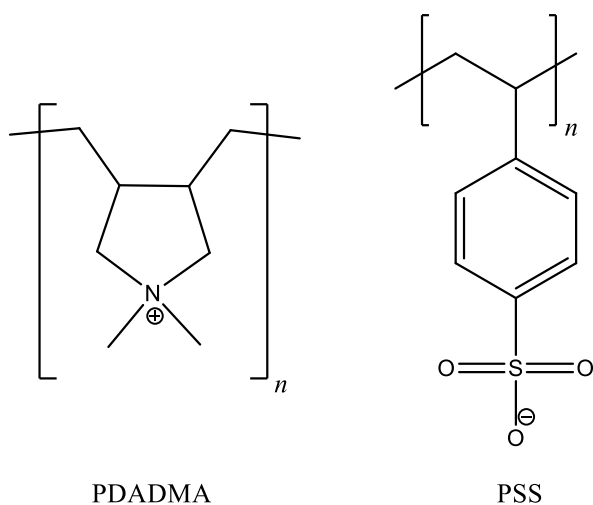


Figure 1.4 Monomer units for poly(diallyldimethylammonium) on left and poly(styrene 4-sulfonate) on right. Both are shown without the respective counterions in order to illustrate areas of charge.

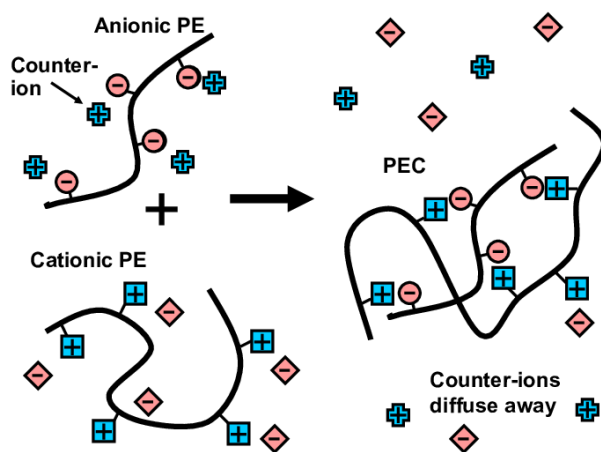


Figure 1.5 A depiction of the formation of PECs within the solution phase.



Figure 1.6 A PEC made using the standard method. Following precipitation, the PEC solid was pressed into a 1 mm deep, 3cm wide washer and allowed to air dry for 24 hours.

Faster and less resource intensive formation of plastics from PECs can be accomplished compared to the formation of other plastics commonly used in thin-film technologies within packaging CO₂ monitoring systems. Large combinations of oppositely charged polyelectrolytes which can be used for the formation of PECs also allows for the selective production of plastics with a variety of characteristics. Plastics can be produced which are more resistant against the effects of gamma irradiation, high heat, and other sterilization techniques commonplace in the medical device industry. Also advantageous to the use of PECs is the ability to change the attributes of the PEC formed with relative ease via the modification of formation conditions; such as the tuning of PEC density through modification of polyelectrolyte reactant ratios and polyelectrolyte chain lengths.¹⁶

Research on the formation of PECs to this point shows considerable dependency on the polyelectrolytes used to form the PEC, as well as the reaction conditions in which those PECs are brought together.^{16,20} Work performed by the Acar group shows little to no dependence of the PEC on the initial molar ratios of the reactant polyelectrolytes, instead almost always favoring close to a 1:1 monomer/charge ratio.¹⁶ Deviance from the 1:1 monomer ratio was found only to be achieved within PECs where the reactant polyelectrolytes had significantly different degrees of polymerization or polymer chain length. Changes in the ratio of cationic to anionic polyelectrolyte charge ratio are significant as density of the PEC is decreased as the ratio strays from a 1:1 monomer composition. Decreased density of the ICPECs might yield porous networks which uptake or release CO₂ more rapidly than those which are of a higher density, effectively achieving a time response mechanism within the ICPEC.

VI. Polyelectrolyte Stabilization of Charged Species

Previous work within this group has shown the ability of polyelectrolyte species to stabilize charged species, such as various pH sensitive indicators, within the solution phase.^{21,22} Within a reducing environment, sulfonate groups on leuco-ITS molecules maintain negative charge. Reduced leuco-ITS is readily re-oxidized under atmospheric conditions from the anionic state to the oxidized ITS form. Addition of PDADMAC to the solution has been shown to increase the stability of the reduced leuco-ITS state, remaining stable for upwards of a week compared to minutes without addition of PDADMAC.^{18,21,22}

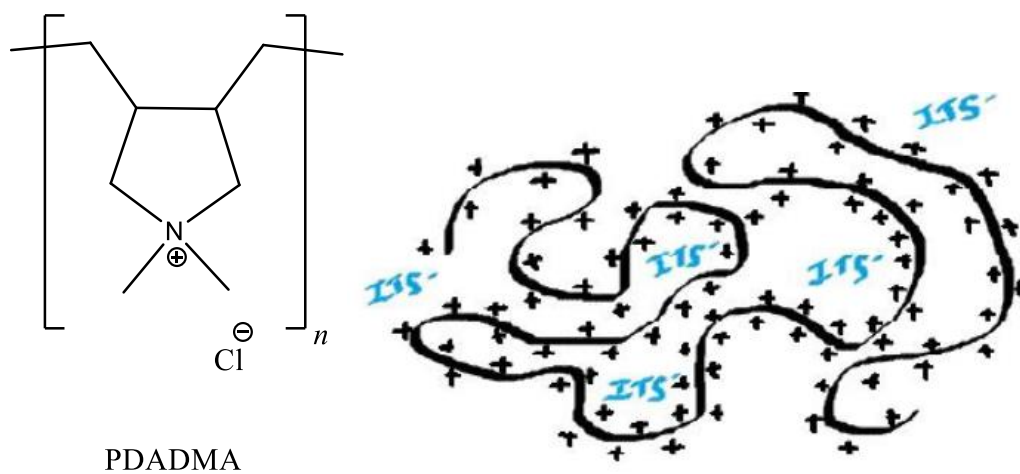


Figure 1.7 On left a monomer unit of PDADMA with the Cl counterion which forms the polyelectrolyte encapsulation of ITS in the leuco form on right.

It is believed that this stabilization of the anionic leuco-ITS species is achieved through interfacial concentration and partial encapsulation within the cationic PDADMA polyelectrolyte present in solution as visualized in Figure 1.7. Coulombic attraction between the ionic species of opposite charge draw both anions of ITS and the reducing agent, in this case sodium bisulfite, against the interface of the cationic PDADMA effectively concentrating the two species and

increasing the rate of reduction. Encapsulation of the two species within the polyelectrolyte lengths also occurs and serves to limit the diffusion of atmospheric oxygen into the system. Kinetic rates established by Hoene characterize this system and the degree to which these species can be stabilized.^{21,22}

VII. Thesis Research

The properties exhibited by pH sensitive species within polyelectrolyte microenvironments show promise for potential use within the field of high concentration CO₂ sensors. In the present study it has been seen that an indicator species, primarily phenol red, can be concentrated in solution using cationic polyelectrolytes. Within a basic environment, the phenol red molecule exists in an anionic form exhibiting a characteristic pink color. Against the interface of the polyelectrolyte the anionic species in solution are brought together and are effectively concentrated as illustrated in Figure 1.8.

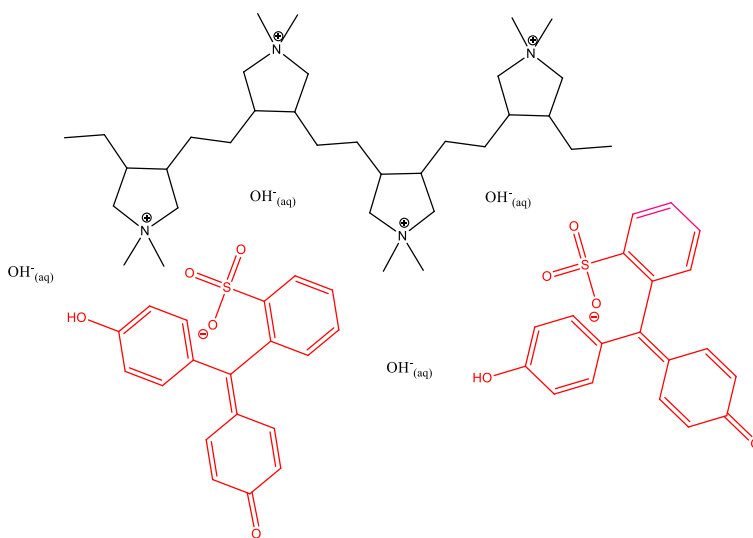


Figure 1.8 Concentration of anionic phenol red against the interface of the PDADMA cationic polyelectrolyte along with the anionic hydroxide species.

Investigation of PECs for various uses, primarily drug delivery systems, is ongoing in many fields of research.²³⁻²⁷ However, no research pertaining to the use of ICPECs as CO₂ monitoring devices is known outside of this research. Investigation of the properties which must be characterized for the practical use of ICPECs within industrial applications were performed. Goals of this characterization include the ability to design ICPECs for application specific needs while maintaining the ease and rapidity of formation which ICPECs achieve over current atmospheric monitoring technologies.

2. METHODS

I. Materials

All reagents used were purchased from Sigma-Aldrich. Polyelectrolytes, purchased and used without treatment or preparation before being diluted to the necessary concentrations, were: poly(diallyldimethylammonium chloride), 20 wt. % in H₂O ($M_w \sim 400,000\text{-}500,000$ g/mol); poly(sodium 4-styrenesulfonate), solid ($M_w \sim 1,000,000$ g/mol); and poly(sodium 4-styrenesulfonate), solid ($M_w \sim 40,000\text{-}70,000$ g/mol). Dyes, purchased and used without treatment or preparation before being diluted to the necessary concentrations, were phenolsulfonphthalein (A.C.S. reagent grade), meta-cresol purple (indicator grade), bromocresol green (A.C.S. reagent grade), thymolphthalein (A.C.S. reagent grade), o-cresolsulfonphthalein (A.C.S. reagent grade), and bromothymol blue (A.C.S. reagent grade). Salts used to create saturated solutions for constant humidity vessels were: lithium chloride ($\geq 99\%$ purity), sodium chloride ($\geq 99\%$ purity), and potassium carbonate ($\geq 99\%$ purity). Bradford reagent was purchased pre-made from Sigma-Aldrich. Hydrochloric acid (37%, A.C.S. grade) was diluted to a usable concentration and combined with anhydrous sodium tetraborate ($\geq 98\%$, puriss. p.a. grade) in order to make a pH 10 buffer for use within the ICPECs. All dilutions were performed using deionized water prepared by an in-house reverse osmosis system.

II. Preparation of PECs

Formation of the ICPECs is accomplished in a manner similar to that which has traditionally been used in the formation of PECs.^{16,19,20,23,28,29} Stock solutions of both PDADMAC and PSSNa were prepared to a concentration of 50 mM so that the monomer ratio of the formed PEC would be ideally 1:1, though this ratio is investigated further within this study to ascertain a more exact

polyanion to polycation ratio. To a beaker 15 mL of both polyelectrolytes are added and the sample is stirred for five minutes to ensure complete complexation of both species.

Approximately 4 mL of this mixture containing both PEC solid and remaining reactants is transferred to each of two containers for centrifugation. Samples are spun in 30 second intervals in a Clay Adams Sero-Fuge 2000 at 3500 rpm with the supernatant being removed before each addition of remaining mixture, until each of the samples had five minutes of collective centrifugation. While it was observed that the initial reaction mixture would precipitate into a solid mass over the course of 24 hours, centrifugation was selected as the method of phase separation due to the more consistent density of the product between trials and the time in which samples could be prepared. Centrifugation was performed after no more than 10 minutes following the addition of the polyanion. Immediately after collection the malleable ICPEC pellets were pressed into an ABS washer and flattened with a microscope slide to a 1 mm thickness to aid in consistency of the dried samples. These flattened samples were then left to dry in open air upon a glass microscope slide.

It was noted during method development that several factors within the PEC and ICPEC preparation could dramatically alter the physical characteristics of the final product. The two largest of these factors was the time the PEC or ICPEC spent within the centrifuge and the time the PEC or ICPEC spent untouched under the remaining supernatant after centrifugation. While these two factors were not investigated, care was taken to ensure sample consistency in light of the ease at which physical characteristics of the samples could be modified by these processes.

III. Preparation of ICPECs

Standard preparation of the ICPECs is performed using a polycation (PDADMAC), polyanion (PSSNa), a buffer solution (boric acid), and a pH sensitive indicator (phenol red). Indicators are integrated into the ICPEC by introducing the selected indicator to the solution containing only cationic polyelectrolytes. Indicators for preparation of ICPECs were selected due to the anionic forms of the indicator which are present within basic conditions. Reaction mixtures are maintained under basic conditions via the utilization of sodium tetraborate decahydrate (borax) buffer which was selected to maintain a pH ~10. Within a basic solution the anionic phenol red species is brought against the interface of the polycationic PDADMAC via Coulombic attraction where it forms an ion pair with the polycation. This reaction mixture containing polycation, pH indicator, and buffering species is referred to in this work as the complex mixture, as it is the solution which will become the ICPEC upon complexation. Upon addition of the polyanionic PSSNa species to the solution, complexation of the polyanion and polycation trap those additional anionic species which are concentrated against the polycation interface.^{28,30-32} Concentration of the anionic species against this strong polycationic interface is believed by this group to occur due to the strong Coulombic attraction which would be present between two oppositely charged ions within solution. This ICPEC is collected as a wet solid via centrifugation of the mixture in the same manner as the previous PECs. Wet solids collected via centrifugation were pressed into 1 mm pellets which maintained relatively uniform dried sample thicknesses within individual sample sets. Samples were allowed to dry for a minimum of one day before any experimentation was performed.

Samples prepared with varying buffer concentrations were prepared largely in the standard manner. Relative buffer concentration gradients were prepared by addition of increased buffer

volume to the complex mixture. In order to maintain a constant volume, samples prepared with lower relative buffer concentrations were diluted with deionized water, as illustrated in Table 2.1. After precipitation of the ICPEC the processing of the product was that of the standard ICPEC. All samples were allowed 48 hours of drying time under laboratory conditions prior to use.

Table 2.1 A general dilution scheme of buffer gradient samples for preparation of ICPECs

Relative Buffer Concentration	Buffer Added (mL)	Water Added (mL)
4x	16	0
2x	8	8
1x	4	12
1/2x	2	14
1/4x	1	15

Samples which were prepared to examine the effects of increasing counterion concentration within the ICPEC reaction mixture were made to have a counterion concentration gradient prior to the addition of the polyanion. Solutions containing polycation, varying buffer, pH sensitive indicator, and various salt concentrations were prepared and then the polyanion was added to form the salted ICPEC. After centrifugation this precipitate was allowed to stand under laboratory conditions to dry for 48 hours. Though it is known that counterions can diffuse through solid PECs when placed into ionic solutions, preparing them with these ions included directly within the ICPEC was done to greatly reduce the time needed for this equilibrium to be established.¹⁹ An example of the counterion concentration gradient within the ICPEC reaction mixture using NaCl is given in

Table 2.2.

Table 2.2 An example of the salt gradient within the ICPEC reaction mixture using NaCl

Total ICPEC Reactant Volume (mL)	Mass NaCl Added (mg)	NaCl Conc. in Reaction Mixture (mM)
49	0	0
49	143	50
49	716	250

Samples which were prepared to examine the effects of variation in atmospheric humidity were prepared using the standard ICPEC formation process utilizing only polycation, pH sensitive indicator, buffer, and polyanion. After precipitation of the ICPEC the samples were treated in the standard manner and dried under laboratory conditions for 48 hours prior to use. Following the initial drying period each of the samples was placed into an atmosphere in which the humidity was known and allowed to equilibrate for an additional 48 hours.

Humidity controlled atmospheres in which the ICPEC samples were placed were prepared using a 200 mm desiccator as an airtight container in which saturated solutions of lithium chloride, potassium carbonate, and sodium chloride were used to create relative humidities of 11.31 ± 0.31 , 43.16 ± 0.33 , and $75.47 \pm 0.14\%$ respectively assuming a constant $20\text{ }^{\circ}\text{C}$ temperature within the laboratory.³³ Samples were placed above the saturated solution within a beaker to allow for equilibration. Sample tubes or containers were also kept within the respective controlled humidity environment. Upon removal of the sample from the controlled humidity environment, the sample would be immediately sealed within the equilibrated sample tube and used immediately for experimentation in order to observe a response which was the most

indicative of the sample behavior within an environment of that relative humidity. While it would be preferable to monitor the time response of the ICPECs directly within the controlled humidity environments, this experimental design could not be achieved using the resources available during the course of this experimentation.

IV. ICPEC Variants

Variants of the ICPEC were attempted which utilized various other pH sensitive dyes as well as other cationic candidates for the replacement of the polycation within the ICPEC. Cationic surfactants benzethonium chloride and cetylpyridinium bromide were each used in the place of the polycation PDADMAC in order to attempt to create a stable PEC or ICPEC from non-polymer species (Figure 2.1). Reaction mixtures containing these cationic species did not form observable PECs and thus could not be used to make ICPECs. Indicators bromothymol blue, *o*-cresolsulfonphthalein, thymolphthalein, bromocresol green, and *meta*-cresol purple were each used in place of phenol red for the formation of ICPECs. Integration of those indicators into the PEC to form the ICPEC was accomplished using each of these indicators, though the sensitivity of these indicators to atmospheric CO₂ concentrations was not seen to be significant in initial study and these ICPECs were not pursued. In the case of the indicator *m*-cresol purple, the time response of the ICPEC was so rapid in early trials that further study was discontinued.

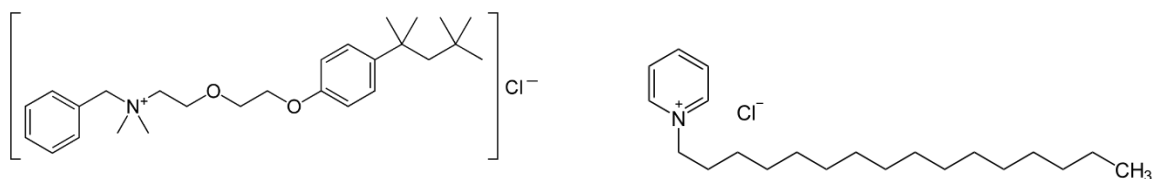


Figure 2.1 Structures of benzethonium chloride (left) and cetylpyridinium chloride (right).

V. Analysis of Internal Moisture Content

Internal moisture content of the ICPEC was experimentally found to significantly affect the time response of the ICPECs upon introduction to high concentration CO₂ environments. This suggest influence on the equilibrium which is responsible for the observed initial color of the ICPEC as well as the timeframe in which the visual transition of the ICPEC occurs when subjected to high CO₂ environments. Work done by the Farhat group showed polyelectrolyte multilayers, formed in a manner which is consistent with the formation of PECs and ICPECs, to have an internal moisture content ranging from 10–20 wt. %.²⁸ Determination of the internal moisture content of ICPECs utilized in this research was performed via use of Simultaneous Thermal Analysis on a Netzsch STA 449 F5. Work performed by the Farhat group showed PDADMAC:PSS PECs are stable when heated above 320 °C and below this point evolve primarily atmospheric moisture as a result of increasing temperature.²⁸ Thermal gravimetric analysis of ICPECs created in this research show similar trends and mass loss. As such, mass loss of the ICPEC below 300 °C was attributed to loss of internal moisture as the sample was heated. Samples were heated from 25 °C to 240 °C at a rate of 20 °C/min and held at 240 °C for 50 minutes in order to drive all loosely bound water from the PEC matrix. Samples held at 240 °C for periods of time longer than 50 minutes showed little additional mass loss and results were truncated to 50 minutes to ensure consistency within sample sets.

Samples which were uniform in composition and prepared under standard atmospheric conditions were analyzed via STA consecutively utilizing the autosampler. Atmospheric conditions within the laboratory were considered constant with regard to relative humidity. Samples prepared in modified atmospheric conditions, i.e. significantly increased humidity, were individually analyzed via STA in order to limit loss of internal moisture to the laboratory

atmosphere via equilibration. Moisture lost through this equilibrium is kept constant relative to the difference between internal ICPEC moisture content and atmospheric humidity by ensuring analysis is performed within the same time constraints between each sample being analyzed.

Also utilized for analysis of the relative moisture content within the surface regions of the ICPECs was a Bruker Alpha FTIR with an installed Platinum ATR module for ATR-FTIR spectroscopy. Samples which were analyzed via ATR-FTIR were broken into small pieces and sampled directly on the surface of the ATR-FTIR crystal. Absorbance of the water stretching modes from $\sim 3300\text{--}3500\text{ cm}^{-1}$ was measured and correlated to the relative presence of water in an ICPEC sample. Baseline and normalization corrections to the IR absorbance spectra gathered were performed using the OPIS software suite which accompanies the Bruker Alpha system.

VI. Time lapse Photography

Upon placement of the dried ICPEC pellet into a sealed high-concentration CO_2 atmosphere, color change indicative of the protonation of the encapsulated indicator is observed within as early as 30 minutes. Visual transition times of the ICPEC from the unprotonated form present within standard atmospheric conditions to the protonated form present within acidic conditions has been observed to be influenced by several characteristic variables such as sample thickness, buffer capacity, environmental moisture content, and internal sample moisture content. To more accurately determine stages at which the transitions begin to occur within the sample, time lapse photography was utilized, an example of which can be seen in Figure 2.2. A Logitech c310 webcam modified for near focus was utilized for time lapse photography against a white sheet of paper for color contrast. Samples were sealed within an airtight plastic bottle which was filled

with CO₂ by simply flowing laboratory grade CO₂ into the container for 30 seconds, removing the filling hose, and quickly sealing the container.



Figure 2.2 Visual transition of phenol red ICPEC within a high CO₂ atmosphere in an eight-hour timeframe.

Points of interest with respect to the visual transition of the ICPEC from the unprotonated to the protonated forms were recorded as the first color change was observed and when color change ceased to occur. Time lapses spanning 72 hours were commonly used as most ICPECs created in this research had complete visual transition within this timeframe. Increments of 30 minutes were commonly used to resolve color change within the ICPECs. Environmental control of the time lapse setup was achieved to the highest degree possible by sealing the ICPEC within an airtight vessel which had been filled with lab grade CO₂ and held at room temperature. Observation of ICPEC re-equilibrium to atmospheric CO₂ concentration was conducted in a similar manner, though the sample was removed from the sealed vessel and placed on a watch glass before observation.

VII. Analysis of Morphology

It has been observed in previous studies, both externally and within this group, that the formation of different morphological features on the surface and within the bulk of the PEC structure can significantly alter the properties exhibited by the PEC.^{13,18,23–26,28} Modification of

the morphological structure of the PEC, and therefore the ICPEC, can be observed via visual inspection after significant compositional differences, such as introduction of ionic compounds to the reaction mixture, are integrated into the PEC.¹⁸ Subtle compositional differences, such as replacement of the indicator within the ICPEC, do not have morphological effects so pronounced as to observe those effects visually. Modification of the porous network present on the surface or within the bulk of the ICPEC is thought to have the potential to modify the absorption rate of atmospheric CO₂ into the structure where it interacts with the encapsulated indicator.

Observation of morphological effects on the surface and within the bulk of the ICPEC structure was accomplished via the use of a FEI Quanta 250 Field Emission Scanning Electron Microscope (SEM) equipped with a Nordlys Nano for Electron Backscatter Diffraction (EDS).

Samples were prepared using a small intact portion of the ICPEC sample. If examination of inner porous networks was being conducted the sample was ground finely within a mortar and pestle. There were two distinct regions of the ICPECs amongst all ICPECs which were prepared. Because of this the top, air dried, side of the ICPEC and the bottom, glass contacting, side of the ICPEC were represented in each sample which was examined on the SEM.

Carbon coating applied via sputtering in ~15 nm thickness was used to ensure conductivity of ICPEC samples after it was determined that resolution of an SEM image could not be achieved due to lack of conductivity within the sample. Parameters used for the SEM were commonly 2 nm spot size, 5 kV accelerating voltage, with a 7 mm working distance. Changes were made to standard operating parameters such as reduction of spot size and accelerating voltage in order to resolve higher order magnifications. Commonly a stage bias of 4 kV was applied in order to reduce charging in areas where current buildup prevented acquisition of images. Images were commonly resolved at 600, 2400, 5000, and 20,000 x magnifications which clearly resolve 100,

20, 10, and 3 μm features respectively. An Everhart-Thornley detector arrangement was utilized for most sample imaging as it allowed for incorporated phase data as well as higher resolution than did the concentric backscatter collector arrangement which was also available.

VIII. ICPEC Analysis of Polyelectrolyte Concentration

It has been shown in previous research that any addition, especially ionic compounds, to the PEC reactant mixture can strongly influence the manner in which the polycation and polyanion come together to form the resulting PEC.^{18,25,34} Ionic forms of the phenol red indicator within the buffered reactant solution, as well as the ionic forms of the buffer itself, pose a possibility of interfering with the formation of the ICPEC. It is thought that interference by ionic addition to the reaction mixture will primarily affect the ratio at which both PECs and ICPECs formed by interactions between PDADMAC and PSSNa. Characterization of this ratio was initially attempted via ATR-FTIR in a manner similar to that which was used to determine polycation/polyanion ratios within coacervate mixtures previously made within this group.¹⁸ Proper resolution of the PDADMAC and PSSNa peaks within the PECs and ICPECs could not be achieved however using ATR-FTIR. Though the ATR-FTIR regions belonging to PDADMAC and PSSNa have been previously used in work by this group to quantify polyelectrolyte concentrations within the coacervate phase, those concentrations found within solid PECs showed to be too concentrated in order to establish relationships which would allow for the determination of polycation to polyanion within the solid. Liquid phases of these polyelectrolytes, even in solutions which had reached complete saturation, were observed to be too dilute to be seen via ATR-FTIR for the purpose of standard curve establishment.

Spectroscopic determination of polymer ratios was instead performed using an Agilent 8453 UV-Vis. It was determined that PSSNa has a strong absorbance at 224 nm and this wavelength was used to establish a calibration curve for the polycation in the liquid phase. Problematic to this approach is the lack of strong absorbance of PDADMAC within the UV-Vis spectrum. Work performed by the Ziolkowska group showed the use of the Bradford reagent, normally used within bioassays, as a binding agent which when bound would absorb strongly at multiple wavelengths within the UV-Vis region.³⁴ Utilizing this method, a polynomial standard curve was established for the PDADMAC-Bradford complex at 590 nm.

As UV-Vis analysis of the polyelectrolyte ratio requires both species to be present in the liquid phase, direct measurement of the polyelectrolyte ratio with the solid PEC could not be made. Instead, the supernatant solution which remains following the precipitation of the PEC or ICPEC was sampled as measurable excess polyelectrolyte remains in the liquid phase. As concentrations of both polycation and polyanion are known prior to complexation an indirect measurement of the PEC or ICPEC polyelectrolyte composition can be made if the supernatant polyelectrolyte concentration can be determined. This method was adapted from a similar method which was used for polycation concentration determination used by the Ziolkowska group.³⁴

Samples were prepared for PSSNa polyanion monomer unit concentration determination by diluting the supernatant 3:100 and observing the 224 nm absorbance. This dilution factor was experimentally determined to best fit the absorbance of the analyte within those ranges predefined within the PSSNa calibration curve. Similarly, the PDADMAC polycation monomer unit concentration determination was performed after a 1:100 dilution of the supernatant solution and observation at the 590 nm wavelength. Because the PDADMAC-Bradford complex had

significant absorption at 224 nm simultaneous UV-Vis data collection of both the polycation and polyanion could not be performed. Polyelectrolyte concentrations were calculated in terms of monomer unit rather than exact polyelectrolyte concentration as complex formation occurs in an ideal 1:1 monomer unit ratio, as well as due to the large molecular weight range present within the stock solutions used. This makes concentrations in terms of monomer units more meaningful in terms of polyelectrolyte complexation.

3. RESULTS AND DISCUSSION

I. Analysis of Internal Moisture and Moisture Uptake

Determination of the internal moisture content of both the PECs and ICPECs was performed in order to examine potential correlation between internal water content and increased sensitivity to high CO₂ environments. Heating curves gained from thermogravimetric analysis performed by the Farhat group gave estimates which were used to determine the breakdown temperatures of the PECs and by extension the ICPECs which were examined.²⁸ Stability of the PEC studied was observed to temperatures of 300 °C in which time no decomposition was observed and only the off gassing of water was present. It was determined that the phenol red indicator used within the ICPECs was also stable up to a temperature of 270 °C, at which point thermal degradation of the indicator was observed. This determination was visually performed within a melting-point determination apparatus.

Utilizing a conservative region within this temperature zone, ICPECs were analyzed via STA up to a temperature of 240°C in order to ensure no thermal degradation of the ICPEC. Mass loss was directly correlated to off gassed water. Examining the sample mass loss as a function of temperature and time as depicted in Figure 3.1, this assumption seems to be valid as very little mass is lost from the sample after the expected diffusion of water from the ICPEC occurs. Trials were run comparing sample mass loss at 240°C over periods of time extending to 3 hours and mass loss regions indicative of sample breakdown or decomposition were never observed. Using this 3 hour trial as a baseline, it was concluded that $94 \pm 4\%$ ($n = 3$) of the sample mass loss due to the diffusion of water from inside the PEC or ICPEC was lost within the first hour when the temperature was held near 250°C. Future samples were then run on much shorter timeframes and this mass correction was applied globally to all samples run using this method. Note that

differential scanning calorimetry (DSC) data was collected alongside the thermogravimetric data using the simultaneous thermal analyzer. While this data was not extensively used, it does show qualitatively in Figure 3.1 that no phases are present, other than the liquid to vapor phase transition of water, which would correlate to the decomposition of the ICPEC. Also note that while there does appear to be a phase transition in the DSC data following the 30 minute time point, this DSC peak is induced by rapid cooling of the sample relative to the reference. Because DSC signal is directly related to the rate at which the reference crucible within the furnace heats relative to the crucible which holds the sample, sudden transitions in temperature ramping can induce DSC signal that would not be observed so significantly with a more gradual temperature ramp.

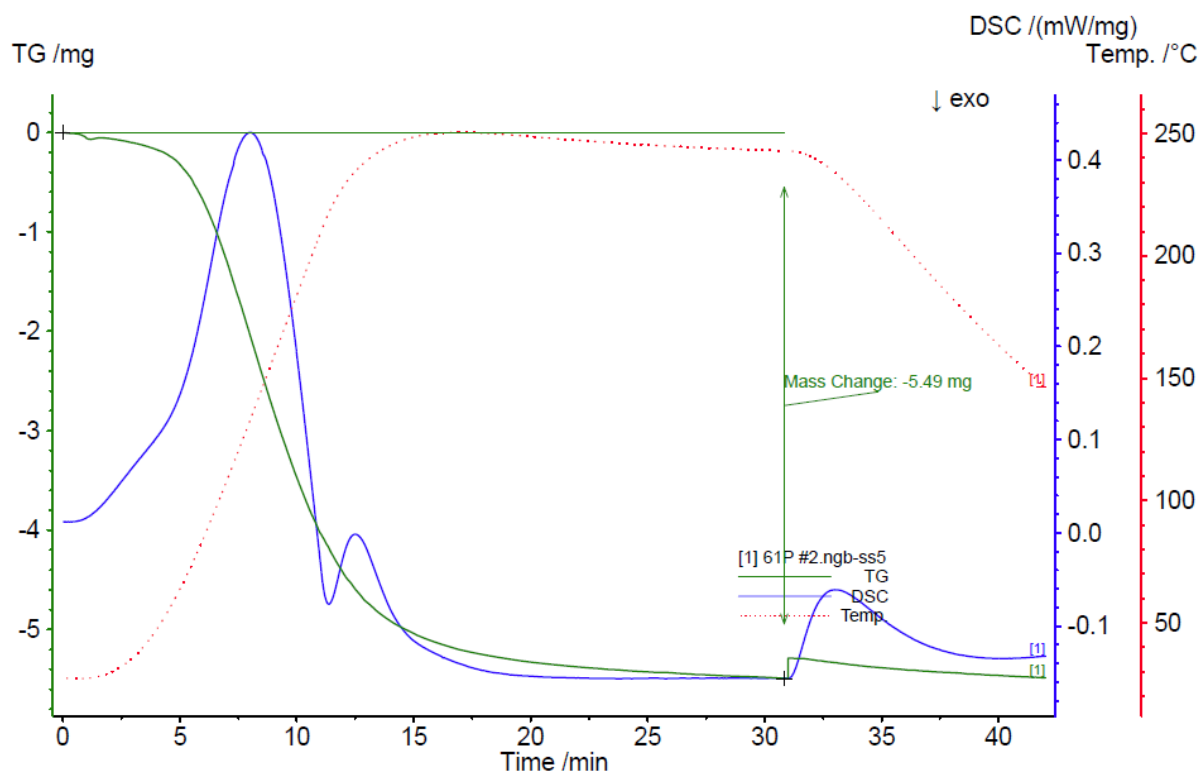


Figure 3.1 STA data showing decreasing mass (green) of the sampled ICPEC as a function of temperature (red) and time. Notice the DSC curve (blue) which was used to establish direct heating endpoints.

It was determined via STA that the standard PEC composed of just polyanion and polycation had an average internal moisture content of $11.2 \pm 0.3\%$ ($n = 3$) by mass (Table 3.1).

Examination of the internal moisture content of the ICPECs revealed that samples prepared using exclusively polycation, indicator, buffer, and polyanion maintained an internal moisture content of $15 \pm 3\%$ ($n = 17$) by mass. Considering the deviation of this second value, the internal moisture of the PEC and ICPEC can be considered compositionally similar as there is no significant difference between the two internal moisture contents. This suggests that introduction of the pH indicator as well as the boric acid buffer used in the composition of the ICPECs did not significantly alter the internal moisture content of these complexes.

Table 3.1 Internal moisture content via % mass loss of standard ICPECs. Note that the elapsed time listed was after the initial 24 drying process. Note the first 17 samples listed are ICPECS prepared with the standard method, and the last 3 samples are PECs prepared with the standard method.

Sample ID	Drying Method	Mass Loss	Days Elapsed Before STA
29P	Air	14.75%	135
46P	Air	19.39%	1
47P	Oven	13.00%	1
48P	Air	13.87%	1
50P	Air	12.93%	0
51P	Air	11.81%	1
52P	Air	12.10%	1
60P	Air	11.54%	1
63P	Air	14.73%	9
63P1	Air	14.99%	23
71P1	Oven	11.54%	17
71P2	Oven	10.08%	17
74P	Air	10.82%	17
81P	Air	12.45%	13
66P	Air	9.48%	6
92P1	Air	7.93%	7
93P1	Air	10.72%	10
96PB 1	Air	11.45%	17
96PB 2	Air	11.37%	17
96PB 3	Air	10.94%	17

Another correlation, however, did become apparent as sampling progressed. All samples, which were dried either by oven or left in open-air, were then allowed to sit in an open-air environment for at least 24 hours before internal moisture content was determined via STA. Relative atmospheric humidity within the laboratory averaged ~40% over the duration of the research period and it is believed that an internal equilibrium was established within the ICPEC. Establishment of the ICPEC internal moisture equilibrium with that of the laboratory environment would yield a constant internal moisture content within the ICPEC given sufficient time to come to equilibrium. Data suggesting this correlation is seen in Figure 3.2, where data has been binned into two day sets in order to achieve error distributions representative of the average internal humidity as a function of time. Points indicated as circles lay outside of the standard deviation of the bulk of the samples within a sample bin. Bins which contained only one sample are represented as lines rather than boxes, in order to indicate that there is no distribution within that bin.

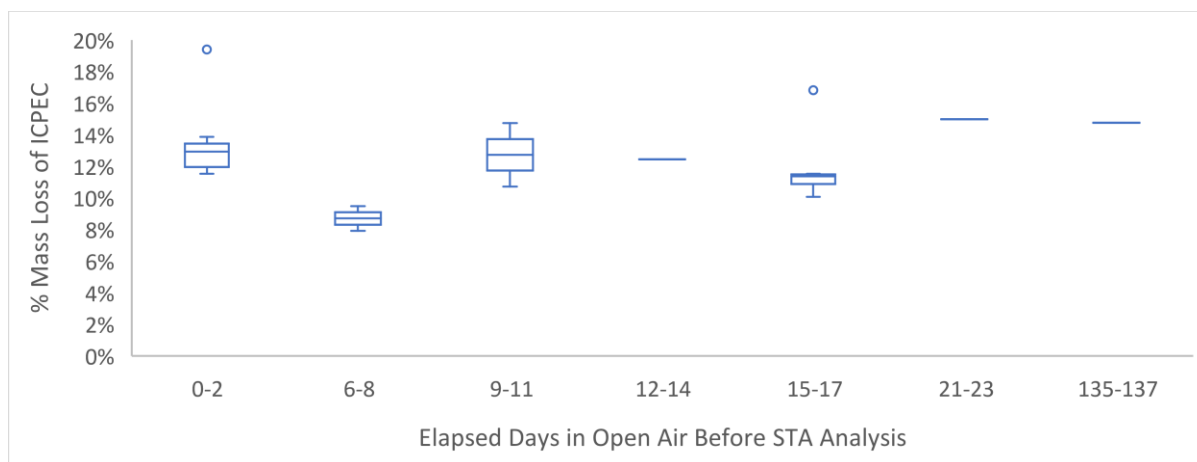


Figure 3.2 Convergence of internal moisture content within ICPECs to atmospheric humidity ~15%. Note the elapsed times listed are in addition to the initial 24 hour drying period.

In Figure 3.2 it is observed that over a large span of time, up to 137 days, ICPECs maintain an average internal humidity of ~13%.

This correlation between the atmospheric humidity and the internal moisture content of the ICPEC suggests rapid uptake of atmospheric moisture by the ICPEC. As seen in Figure 3.2 this can be observed to occur in as little as 24 hours after creation of the ICPEC from the solution phase (Table 3.2). It is also observed that additional drying does not occur after the initial 24 hour drying period, implying that this rapid establishment of the initial drying is indeed the final equilibrium under laboratory conditions after which the internal moisture of the ICPEC remains constant. Samples shown in Table 3.2 were initially dried for 48 hours prior to use, and then allowed to come to equilibrium within the controlled humidity environment for an additional 48 hours before being analyzed via STA or ATR-FTIR. Values for Δ Date represent the difference in time between the sample being removed from a controlled humidity environment and being sampled by TGA.

Table 3.2 Internal moisture content of the ICPECs after being subjected to an atmosphere with a constant relative humidity for a 48 hour equilibration period. LiCl, K₂CO₃, and NaCl generate atmospheres with relative humidities of 11%, 43%, and 75% respectively. Note all elapsed times before sampling are after the 24 hour initial drying period and the 48 hour atmospheric subjection period.

Sample ID	Relative Humidity	Mass Loss (%)	ΔDate
76P	43%	10.1%	17
81P	11%	10.9%	13
86P	75%	17.7%	11
87P	43%	10.7%	6
87P	11%	10.1%	6
87P	75%	18.6%	6
95PB1	11%	11.2%	9
95PB2	43%	16.4%	9
95PB3	75%	<i>Unknown</i>	<i>Unknown</i>

After subjection of three sample sets, comprising nine total samples, to STA for examination of internal moisture content via total % mass loss it was determined that the data suggests there is a range in which a linear correlation exists between the internal moisture content of an ICPEC and the relative humidity of the atmosphere in which the ICPEC was equilibrated as is seen in Figure 3.3.

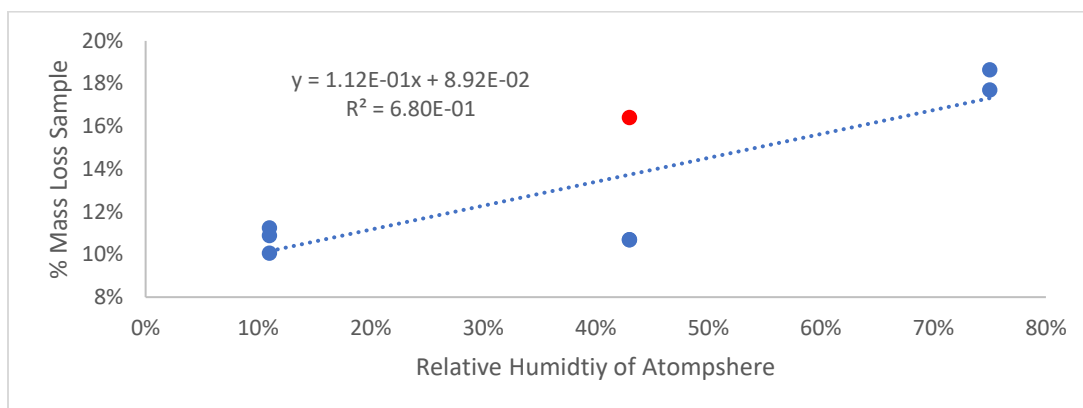


Figure 3.3 Relationship between internal water content of sample and the relative humidity of the atmosphere in which the sample was placed. Note the point (red) which corresponds to proper preparation of the K_2CO_3 saturated solution.

It is immediately apparent that the correlation constant of 0.653 between the relative humidity of the atmosphere and the internal moisture content of the ICPEC samples is lower than would be desired. Relative humidities produced by the K_2CO_3 saturated solutions (43% rel. humidity) were initially observed to be substantially lower than those which were being observed in the ICPECs.

Further research on the preparation of saturated solutions, specifically K_2CO_3 , revealed that it is common for density regions to exist in saturated salt solutions which would influence the rate of vaporization, and therefore the relative humidity achieved, in saturated solutions where a layer of liquid water resides across the entire surface of the undissolved solid. To remedy this the

saturated K_2CO_3 solution was prepared as a “solid slurry” where dry K_2CO_3 was heaped into a small beaker and water was added to wet the K_2CO_3 solid until the volume of water needed to fill the entire volume of the sealed chamber with water vapor was achieved. The volume of water needed was determined using an overestimation via the ideal gas law in a sealed chamber with an estimated volume of 1 L. In the final saturated K_2CO_3 solution solid K_2CO_3 was present both above and below the surface of the water, allowing direct interface of the wetted solid with atmospheric humidity to establish the initially desired equilibrium.

This correction in the preparation of the K_2CO_3 saturated solution was applied to sample 95PB 2 which corresponds to the outlier point (red) in Figure 3.3. Omitting this point from the graph yields Figure 3.4 in which the correlation between relative humidity of the atmosphere and the internal moisture content of the ICPEC are more strongly correlated with a coefficient of 0.941. This correlation, while limited in range, allows for determination of the internal moisture content of the sample within most atmospheres in which the pH sensitive indicator would be utilized. This is especially useful for the practical application of the ICPEC given that internal moisture content of the ICPECs is shown within this research to correlate to the time response of the ICPEC to introduction to CO_2 .

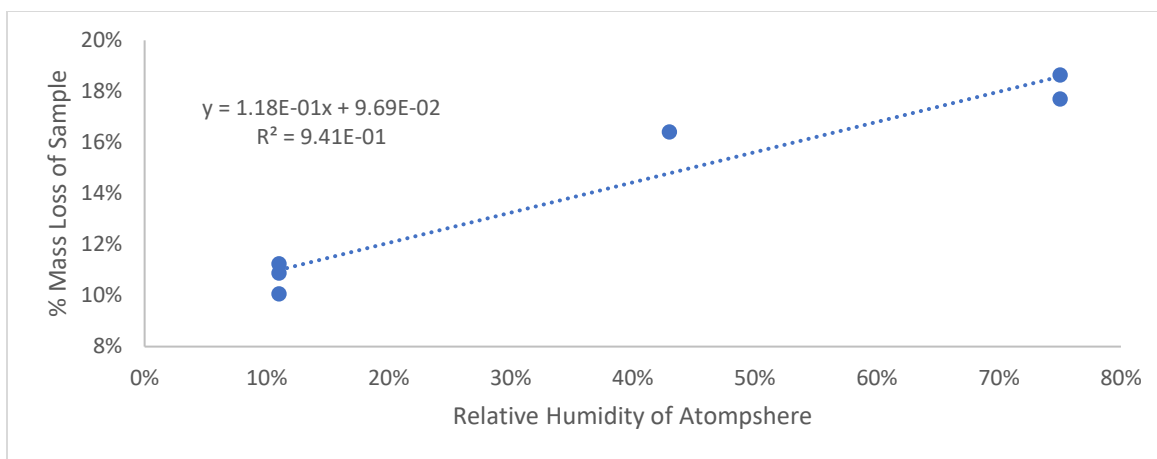


Figure 3.4 Corrected correlation between internal moisture content of the ICPEC and the relative humidity of the atmosphere in which the ICPEC was equilibrated.

II. Time lapse Studies

Time lapse studies of individual ICPECs utilizing the indicators phenolsulfonphthalein (phenol red), *meta*-cresol purple, bromocresol green, thymolphthalein, *o*-cresolsulfonphthalein, and bromothymol blue showed only ICPECs containing the phenolsulfonphthalein indicator or *m*-cresol purple to be readily useful for delayed time response use. Time responses of the indicators *o*-cresolsulfonphthalein and bromothymol blue showed complete color change in less than thirty minutes which did not allow for evaluation of utility as a CO₂ sensitive device which could have time resolutions over a 48 hour period. In the case of thymolphthalein and bromocresol green, no color change was ever observed within ICPECs which utilized these indicators. Also, in the case of thymolphthalein, ethanol additions were required for full dissolution of the indicator into the reactant mixture which led to structural compromise of the resulting ICPEC in the few cases where precipitation of the ICPEC could be achieved.

Time response of an ICPEC was qualitatively determined at two points; the point at which the sample started to transition in color, and the point at which the color transition had been completed. Time response of the ICPECs when introduced or removed from high concentration

CO₂ environments was studied in to 107 samples utilizing the phenol red indicator, 12 samples of *m*-cresol purple, and close to 15 of various other compositions. Sample ICPECs which contained the phenol red indicator had the most distinct visual transitions, were the most reproducibly prepared, and created ICPECs which were accepting of various additions to the overall composition that were being studied. Solubility of phenol red in the basic complex mixture being much higher than the other pH indicators used is largely attributed to the increased utility of this indicator within the ICPECs. Select phenol red samples which illustrate the scope of these time lapse studies are listed in

Table 3.3.

Table 3.3 Various samples and their listed time responses to CO₂ exposure. Samples ID's are roughly indicative of chronological order. All listed samples utilized the phenol red indicator within the ICPEC. % Humidity refers to the humidity of the atmosphere which the samples were exposed after drying.

Sample ID	Drying method	Composition	Initial Response	Final Response
28P	Oven	Standard	2 h	48 h
29P	Air	Standard	2.5 h	6.25 h
30P 1	Air	Standard	1.5 h	7 h
30P 2	Air	Standard	2 h	11 h
38P	Air	Standard	1 h	5 h
39P	Oven	Standard	1 h	9 h
40P	Air	50 mM NaCl	3 h	40 h
41P	Oven	50 mM NaCl	7 h	< 72 h
44P	Air	Standard	2.5 h	6.25 h
45P	Oven	Standard	2.5 h	6.25 h
63P	Air	Standard	1 h	8.75
64P	Air	10 mM NaCl	15 h	< 72 h
65P	Air	50 mM NaCl	Unknown	Unknown
80P	Air	Standard	3 h	12 h
83P	Air	4 x Buffer	5 h	< 72 h
84P	Air	Standard	5 h	< 72 h
85P	Air	1/2 x Buffer	5 h	< 72 h
91P1	Air	11% Humidity	2 h	< 72h
91P 2	Air	43% Humidity	2 h	10 h
91P 3	Air	75% Humidity	> 0.5 h	0.5 h
91P 4	Air	11% Humidity	5 h	< 72 h
91P 5	Air	43% Humidity	1.5 h	8 h
91P 6	Air	75% Humidity	> 0.5 h	1 h
92P 1	Air	Standard	13 h	33 h

92P 2	Air	50 mM NaCl	23 h	46 h
92P 3	Air	250 mM NaCl	95 h	Not Observed
94P 1	Air	$\frac{1}{4}$ x Buffer	0.5 h	3 h
94 P 2	Air	$\frac{1}{2}$ x Buffer	0.5 h	3 h
94P 3	Air	Standard	3 h	7 h
94P 4	Air	2 x Buffer	3 h	15 h
94P 5	Air	4 x Buffer	3 h	25 h

Phenol red ICPECs show average time responses of 2.5 hours to initial color change and upwards of 7 hours to complete color change within the ICPEC (

Table 3.3). While performance of the phenol red ICPECs averaged initial time responses of 2.5 hours and final responses of 7 hours, any variation of the ICPEC preparation or composition was immediately seen to change the responsiveness of the material. Many factors which control the time responsiveness are still to be identified. While considerable variation of up to 4 orders of magnitude between time responses was observed with the sample composition and preparation method, relative time responses within sample sets were clearly identified. While this variation in the time-response limits the utility of this preparation method for use as a high concentration CO₂ indicator with a predictable time response without further study, it does still allow for the characterization of the ICPECs from a relative standpoint and for observation of the effects of various compositional modifications.

Speculation concerning the factors which may control sample characteristics and cause variation in the sample behavior between sample sets is based largely on what is already known about the PECs and would therefore also apply strongly to ICPECs. During the formation of a PEC counterions are expelled from the interface of the two polyelectrolytes. As these counterions become dissociated from the polyelectrolytes and as the polyanion and polycation come together to become more charge neutral, the solubility of the newly formed PEC decreases significantly causing precipitation. Because the formation of the PEC is favored due to the

entropically driven expulsion of counterions from the polyelectrolytes, the resulting PEC does not necessarily maintain a net negative charge due to polyanion/polycation charge cancelation.¹⁷⁻

¹⁹ Counterion/polyelectrolyte pairing still exists at PEC/water interfaces both on the outer surface of the precipitate and within the PEC due to the significant internal water content.²⁸ Locations within the PEC where charge balance is maintained through polyanion/polycation pairing are referred to as intrinsic sites while locations where charge balance is maintained through cation/polyanion or anion/polycation pairing are referred to as extrinsic sites as is visualized in Figure 3.5.¹⁷ Regions high in intrinsic sites within the PEC are well known to be very dense with significant polyelectrolyte interpenetration while extrinsic sites, especially within the PEC, cause significant swelling of the PEC and reduction in density. Further addition of ions to the PEC system will result in lessening of the PEC density due to the creation of these extrinsic sites within the complex. This creates a density gradient as a function of ion concentration, a portion of which is represented in Figure 3.6. This is in part due to the hydration sphere of the ion which is present around these counterions while solvated as well as the charge repulsion present between counterions and nearby non-compensated polyelectrolytes. This ionic swelling is known to be responsible for the creation of coacervate systems from PECs as the counterion/polyelectrolyte mixture reaches a critical point along this gradient.^{17-19,32}

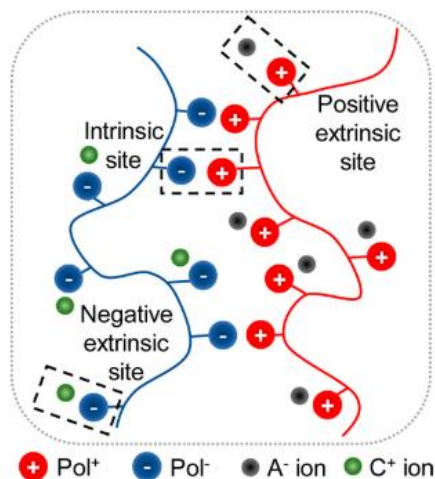


Figure 3.5 Net neutral charge maintenance by both extrinsic charge coupling (left and right boxes) and intrinsic charge coupling (middle box).¹⁷

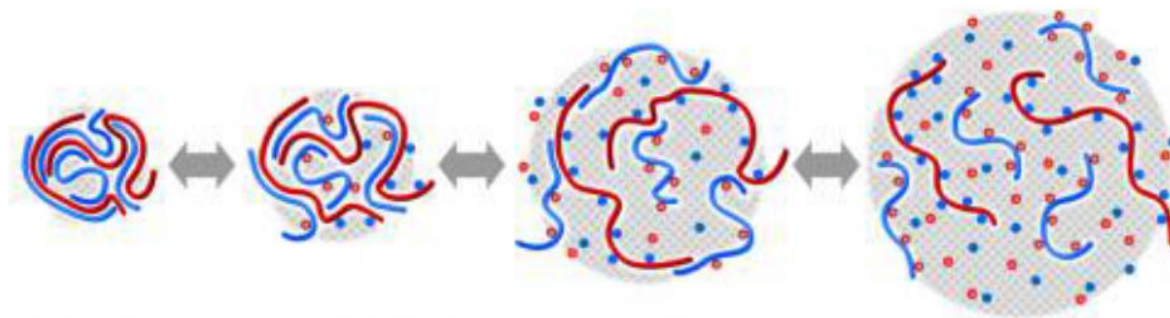


Figure 3.6 A visualization of the density gradient present within a PEC as counterions are added to the complex mixture where anions and polyanions are shown in red and cations and polycations are shown in blue. (counterion concentration increases from left to right).¹⁹

Kinetics of counterion expulsion from within the PEC are non-trivial even in thin PEC films or polyelectrolyte multilayers only several nanometers in thickness.^{20,24,35,36} General understanding of these kinetics though would certainly insist that the rate at which the polyelectrolytes which form the PEC come together paired with the rate at which the counterions were allowed to diffuse from extrinsic sites would dramatically alter the density and therefore the porosity of the PEC or ICPEC in this case. Rapid introduction of the polyanion to the complex mixture without allowing time for the system to come to equilibrium could lead to trapped states in which more extrinsic sites exist than would normally under complete equilibrium. If this

speculative explanation were to hold true in the case of the prepared ICPECs then uncontrolled rates of polycation and polyanion addition via various delivery methods might yield ICPECs which have largely different polymeric compositions and densities.

This explanation might also yield insight as to why the behavior of centrifuged ICPECs also had significantly different physical properties than those allowed to simply precipitate under standard conditions. Separation of the precipitate and solution phase by relative density may yield regions within the PEC in which the entropic complexation of the two polyelectrolytes is forcibly shifted either toward or away from equilibrium conditions, either of which persist due to otherwise slow counterion diffusion through the PEC. As internal water within the PEC is driven out via gravimetric separation polyelectrolytes would likely shed extrinsic pairs and the degree of polyelectrolyte interpenetration would increase due to the need for charge compensation. This trend is indeed observed, though increased density of precipitate following centrifugation is hardly unique to the centrifugation of ICPECs.



Figure 3.7 Two phenol red ICPECs where one is air dried (left) and the other is dried at 70 °C for 1 hour before being air dried (right).

Table 3.4 Phenol red ICPECs sample sets designed to compared drying temperature and time response.

Sample ID	Drying method	Composition	Initial Response	Final Response
28P	Oven	Standard	2 h	48 h
29P	Air	Standard	2.5 h	6.25 h
38P	Air	Standard	1 h	5 h
39P	Oven	Standard	1 h	9 h
44P	Air	Standard	2 h	6.25 h
45P	Oven	Standard	2.5 h	9.5 h

Seen in Table 3.4 are three phenol red ICPEC sample sets, comprising six total samples, which showed correlation between drying temperatures and the CO₂ initial response times of the ICPEC. Each of these heat-treated samples showed significantly delayed time responses when subjected to high CO₂ concentrations and less overall color reversibility when removed from a high CO₂ environment. Samples which have been dried at higher temperatures were found to be very fragile, thin, and morphologically distinct as seen in Figure 3.7. Variation in the time responses between sample sets did not allow for a direct relationship between drying temperature and time response to be established. Time response in oven dried samples relative to air dried samples were observed to increase between roughly 50–750%. The oven used to dry samples in quantities which might be studied by time lapse has limited temperature control in the low ranges which were utilized for drying of the ICPECs (> 70 °C). As samples which were prepared identically, oven dried for the same period of time at the same temperature, and allowed to sit under atmospheric conditions for the same period of time had CO₂ response times which varied from 2 hours to 5 hours, it was concluded that limited temperature control of the oven used paired with variable humidity in the laboratory setting was responsible for considerable variation in sample response to introduction of CO₂. Relative comparison between air dried and oven dried samples from the same set does indicate that heat treatment of samples does increase the time response of the ICPEC when introduced to high concentration CO₂ environments.

Degradation in time response of these samples is believed to be due to loss in internal moisture within the ICPEC. As internal water is expelled due to increased drying temperatures aggregate regions within the ICPEC, in which buffering and pH indicator species are present, lose volume and therefore become more concentrated. Increased concentration of the buffering species yields aggregate regions which would require increased diffusion of CO₂ in order to achieve protonation of the pH indicator species. This concentration might be significant enough in magnitude that the boric acid buffer would no longer be considered solute. A sharp increase in activity is known to correspond to increased ionic strength over ~0.1 M, concentrations which might be present within these concentrated aggregate microenvironments. Environments such as this would yield non-linear correlations between the buffer capacity and the amount of diffused CO₂ necessary to elicit a predictable time response from the pH, which was experimentally observed as seen in Table 3.2.

Compounding this effect would be the tendency of internal water within the ICPEC to be increasingly present in regions more near to the surface. The presence of increased moisture near the surface regions of the ICPEC is due to extrinsic pairing between counterions and the polyelectrolytes which is likely to yield hydrophilic regions within the ICPEC structure. These structures would likely exist against the surface as they are formed in solution. As ions are entropically diffused from the more internal portions of the ICPEC due to the intrinsic pairing for the polyelectrolytes, the ability of water to be maintained within these regions via ion-water pairing is also reduced. As a result, ion-water pairs migrate to the surface regions of the ICPEC where charge balance can be more easily achieved via interpenetration and equilibrium overcompensation within the ICPEC itself.^{17,20}

Experimentally this migration of internal moisture was observed within the ICPEC via ATR-FTIR in an initial attempt to establish a linear relationship between internal moisture content of the ICPEC and the absorbance at the water stretching modes $\sim 3300\text{--}3500\text{ cm}^{-1}$. In order to determine if water loss of the sample could be observed as a function of drying time, a wet sample given less than the standard 24 hour drying period was examined via ATR-FTIR and STA and then every 24 hours for a period of 72 hours in total. This wet sample was prepared to produce three identical subsamples each of which was divided in two, half for STA analysis and half for ATR-FTIR, after the shortened drying period following the separation of the solid ICPEC from solution. Each absorbance value reported for ATR-FTIR is representative of the average of four ATR-FTIR measurements following baseline correction and normalization within the OPIS software suite. Averaging was done to account for potential differences within the surface structure of the ICPEC.

Seen in Table 3.5, it was observed via STA that though the mass loss associated with the removal of water from the ICPEC increased initially and held constant after the initial drying period of 24 hours was reached. Observed in the ATR-FTIR absorbance spectrum however was an increase in the absorbance of the $\sim 3300\text{--}3500\text{ cm}^{-1}$ region as a function of time, corresponding to an increased presence of water in aged samples (Figure 3.8).

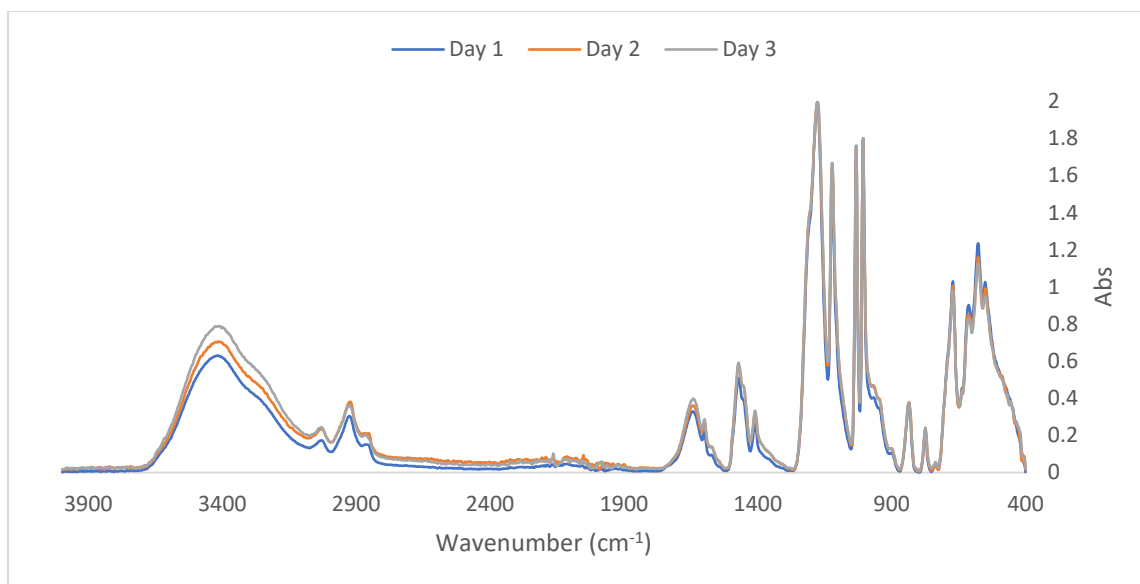


Figure 3.8 Absorbance data gathered via ATR-FTIR over three days of the ICPEC sample 66P examining the increase in the absorbance associated with water stretching modes as a function of time.

Table 3.5 Percent mass loss gathered via STA and absorbance of water stretching modes in the IR spectrum.

Sample Age (Days)	% Mass Loss of Sample	Absorbance 3400 cm ⁻¹
1	11.62	0.61969
2	9.46	0.699385
3	9.48	0.781465

Infrared spectra gathered via ATR-FTIR only represents those molecules which are allowed to interact with the evanescent wave which is propagated by the IR source within the instrument. Penetration depth of this wave is variable depending largely on the refractive index of the material being sampled, though this depth normally is limited between 0.5–3 μm . Penetration depth of this magnitude would only allow for interaction of the molecules representative of the surface layer of the ICPEC to be sampled via ATR-FTIR without further sample treatment. From this observation we can surmise migration of internal water to the surface of the ICPEC from within the ICPEC is occurring as a function of time. Migration of internal water to the surface is

thought to assist in the rapid dehydration of these samples which is observed once removed supernatant solution after complexation.



Figure 3.9 Three phenol red ICPECs prepared from counterion solutions with concentrations 250 mM (left), 50 mM (center), and 0 mM for control (right)

Table 3.6 Phenol red ICPECs sample sets designed to compare counterion concentration in complex mixture and time response.

Sample ID	Drying method	Composition	Initial Response	Final Response
40P	Air	50 mM NaCl	3 h	40 h
41P	Oven	50 mM NaCl	7 h	< 72 h
63P	Air	Standard	1 h	8.75
64P	Air	10 mM NaCl	15 h	< 72 h
65P	Air	50 mM NaCl	Unknown	Unknown
92P 1	Air	Standard	13 h	33 h
92P 2	Air	50 mM NaCl	23 h	46 h
92P 3	Air	250 mM NaCl	95 h	< 120 h

Seen in Table 3.6 there were three phenol red ICPEC sample sets, comprising eight total salted samples, showed correlation between ionic compound addition and CO₂ introductory response times of the ICPEC. Addition of sodium chloride to both oven and air-dried phenol red ICPECs consistently increased the time response of the ICPECs to CO₂ introduction roughly two-fold. These ICPECs were observed to be reversible for at least two cycles, though the dramatically increased time response of these samples limited the observation of this cycling to one sample. Time response to introduction to CO₂ increased two to five-fold between the standard and 50 mM NaCl samples, and upwards of four-fold between 50 mM and 250 mM

samples. Variability encountered in the air-dried sample sets was inherited largely from the different physical properties ICPECs inherit as a function of increased ionic uptake.

Work done within this group by Kaiser, as well as significant work outside the group, have shown ionic additions to PECs can significantly disrupt equilibrium by which entropic favorability holds the polyanion and polycation together.^{18,28,32,36,37} During the formation of the PEC it is accepted that diffusion of the counterions occurs as the polyanion and polycation come together in an enthalpically more stable complex. Additional counterions present within the reaction mixture create a new equilibrium which favors a larger presence of counterions within the PEC and therefore can dramatically change the physical properties of the PEC. These counterions and accompanying hydration spheres cause a swelling of the outer layers of the PEC. By extension the physical properties of the ICPEC are anticipated to change in a similar manner, and this is observed within the sample sets.

Phenol red ICPEC samples prepared under standard conditions precipitate from solution slowly within one hour from the time of the polyanion addition. Upon drying these samples have a smooth appearance, are relatively fragile, and retain much of the shape imparted by the circular washer into which the wet ICPEC pellet was pressed. When ICPECs were prepared from solutions with increasing concentration of counterions present prior to polyanion addition physical changes in the ICPEC were immediately noted.

Increasing counterion concentration within the solution led to an apparent increased volume of precipitated ICPEC due to a substantial decrease in the density of the precipitated ICPEC. Upon drying, ICPECs formed in solutions with larger concentrations of counterions were observed to contract dramatically relative to the contraction observed in the ICPECs prepared by the standard method. These ICPECs formed within strongly ionic solutions were much less

malleable, often requiring a great deal of force in order to be shaped into the washer used to mold consistent samples.

Contraction of the ICPECs was observed in all samples, though this effect was greatly increased as the concentration of counterion used in preparation was increased. This effect is clearly demonstrated in Figure 3.9 as the counter ion concentration within the complex mixture used for preparation of the ICPEC increases from right to left. Dried samples were greatly distorted from the molded shapes, rough in appearance, increased in thickness on average ~50%, and were much more resistant to breakage than those samples prepared without counterion addition.

Correlation between increased sample thickness, increased counterionic strength in the complex mixture, and increased time response to introduction of CO₂ was well established. Initially it was proposed that increased thickness of the sample limited the rate at which diffused CO₂ could interact with the encapsulated indicator. Analysis via SEM elucidated a potentially more viable mechanism for decreased sensitivity to atmospheric CO₂ however resulting from the decreased porosity of the ICPEC surface as a function of counterionic addition (see Section III).



Figure 3.10 Three of five phenol red samples in the 94P sample set showing 1x buffer composition (left), 2x buffer composition (center), and 4x buffer composition (right). ICPECs with 1/2x and 1/4x buffer concentrations formed thin films which weren't able to be photographed in whole samples due to fragile composition. Note the increase in the reflective surface of the ICPECs from left to right.

Table 3.7 Phenol red ICPECs sample sets designed to compare increased buffer addition in complex mixture and time response.

Sample ID	Drying method	Composition	Initial Response	Final Response
83P	Air	4 x Buffer	5 h	< 72 h
84P	Air	Standard	5 h	< 72 h
85P	Air	$\frac{1}{2}$ x Buffer	5 h	< 72 h
94P 1	Air	$\frac{1}{4}$ x Buffer	0.5 h	3 h
94 P 2	Air	$\frac{1}{2}$ x Buffer	0.5 h	3 h
94P 3	Air	Standard	3 h	7 h
94P 4	Air	2 x Buffer	3 h	15 h
94P 5	Air	4 x Buffer	3 h	25 h

Table 3.7 shows two phenol red ICPEC sample sets, comprising six total samples with varied buffer concentrations. A correlation is seen between increased buffer addition and CO₂ initial response times of the ICPEC, where increasing effective buffer capacity increases time-response to CO₂ introduction. Samples from the 94P sample set are shown in Figure 3.10 for comparison of morphology. The boric acid buffer is used to maintain an internal pH 10 within the ICPEC under atmospheric conditions. Internal formation of H₂CO₃ via diffusion of CO₂ into ICPEC is believed to be responsible for the transition of the encapsulated phenol red indicator from the deprotonated to the protonated form. Increasing the concentration of the boric acid buffer within the reaction mixture prior to the addition of the polyanion effectively increases the buffer

capacity of the precipitated ICPEC; therefore increasing the concentration of diffused CO₂ which must be present in order for the encapsulated indicator to transition to the protonated form.

Effective buffer capacities of 4x, 2x, 0.5x, and 0.25x relative to the standard ICPEC buffer concentration were achieved in the reactant solution prior to addition of the polyanion by reducing the concentration of the boric acid buffer by an equivalent factor, though true buffer capacity via buffer titration was not performed. Observed in ICPECs prepared with reduced buffer capacities was a non-linear decreased time response upon introduction to CO₂, though sufficient data to establish a more direct correlation was not collected. In one sample set effective buffer capacities of 4x, 2x, 0.5x, and 0.25x yielded time responses which were roughly 400, 200, 50, and 50% respectively of the standard ICPEC from the same batch to which the samples were compared. Some samples prepared with effective buffer capacities 2x or greater did not yield ICPECs which could be utilized for CO₂ detection as time response to introduction of CO₂ was never observed. These samples were observed to dry in a manner which was not consistent with samples of the same composition with a lesser effective buffer capacity, were often strongly discolored, and no response was observed upon introduction of CO₂ within these ICPECs. Samples made with buffer capacities less than ¼ that of the standard ICPEC were observed to irreversibly change color upon exposure to CO₂. Above the effective buffer capacity of the standard ICPEC solid boric acid precipitate was apparent within the buffer solution which would readily dissolved upon addition to the reactant mixture.

While dissolved in the reactant mixture, anions within the more concentrated buffer are speculated to concentrate further against the interface of the polycation present within solution. Precipitation of the ICPEC from solution upon addition of the polyanion may yield aggregate regions within the ICPEC in which concentration of the buffer ions is once again increased to the

point of precipitation. Within the solid ICPEC these buffer aggregate regions, accompanied by encapsulated moisture, would be sufficient to maintain a high internal pH with a large buffer capacity. Under atmospheric pressures internal concentration of H_2CO_3 would not be significant enough to facilitate the transition of the encapsulated indicator to the protonated form, even within extremely high concentration CO_2 environments.



Figure 3.11 Two phenol red ICPECs having been exposed to atmospheres with controlled humidities for 48 hours. The ICPEC which was exposed to a 75% relative humidity (left) appears much more translucent and brighter in color than the ICPEC dried in a 11% relative humidity (right).

Table 3.8 Time responses of various phenol red ICPECs as a function of the controlled humidity to which each sample was exposed to prior to time lapse photography.

Sample ID	Drying method	Composition	Initial Response	Final Response
91P1	Air	11% Humidity	2 h	< 72h
91P 2	Air	43% Humidity	2 h	10 h
91P 3	Air	75% Humidity	> 0.5 h	0.5 h
91P 4	Air	11% Humidity	5 h	< 72 h
91P 5	Air	43% Humidity	1.5 h	8 h
91P 6	Air	75% Humidity	> 0.5 h	1 h

Table 3.8 shows the results of one phenol red ICPEC sample set, comprising six total samples, in which the samples 91P1 – 91P3 were subjected to an atmosphere with a controlled humidity for 48 hours before the time response was measured, and samples 91P4 – 91P6 were kept under controlled relative humidity conditions for close to two weeks and are seen in Figure

3.11. Two sample sets were prepared from the same initial batch in order to attempt to verify that the ICPECs from the first batch had come to equilibrium with the atmospheres in which they were placed. It can be seen that those ICPECs which were subjected to environments with higher relative humidities have a considerably more rapid time response to the introduction of CO₂. In the case of the 75% humidity samples the initial time response was often so rapid that this transition was not observed in the 30 minute time lapse range. While this trend is observed in all samples in which time response was observed as a function of prior atmospheric relative humidity, this relationship remains relative due to considerable variation in the behavior of individual sample sets and the qualitative nature of the correlation data which was gathered. This effect is seen to verify those explanations which correlate internal moisture to increased interaction between pH sensitive indicators and decreased buffer capacity within the aggregates responsible for color change within the ICPECs.

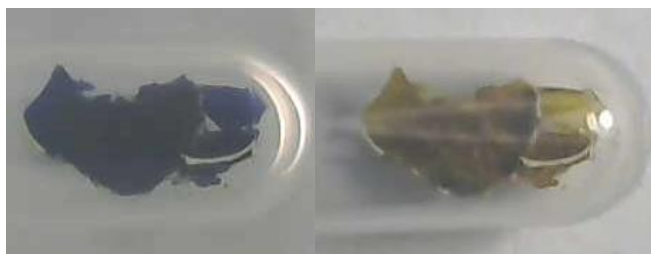


Figure 3.12 One m-cresol purple ICPEC shown before (left) and after (right) exposure to a high CO₂ environment for 50 hours.

Table 3.9 Samples which utilized m-cresol purple as the pH sensitive indicator and the response times of those samples.

Sample ID	Composition	Buffer System Used	Initial Response	Final Response
3M	<i>M</i> -Cresol Purple	Ammonia	2.5 h	10 h
4M	<i>M</i> -Cresol Purple	Ammonia	3 h	10 h
8M	<i>M</i> -Cresol Purple	Ammonia	1 h	4 h
9M	<i>M</i> -Cresol Purple	Ammonia	1 h	3 h
11M	<i>M</i> -Cresol Purple	Boric Acid	4.5 h	46 h
12M	<i>M</i> -Cresol Purple	Boric Acid	4 h	50 h

Table 3.9 describes results from three sample sets, comprising six total samples, which utilized the pH sensitive indicator *m*-cresol purple. Future work aims to study ICPECs which utilize this indicator, as these ICPECs show time response to introduction of CO₂ within a precise range with clear visual response as is seen in Figure 3.12. It should be noted that samples 3M, 4M, 8M, and 9M all utilize the ammonia-ammonium buffer which was used initially during the course of research. Use of the ammonia-ammonium buffer system was largely discontinued due to concerns relating to the reversibility of those ICPECs which were prepared with this buffer system. It was thought that the buffer systems which utilized larger and less volatile components might yield more stable buffer capacities within these systems after introduction to high concentrations of CO₂.

III. Morphological Studies

Examination of the fine morphological structure of the PECs and ICPECs was conducted in order to attempt to correlate the degree of porosity present within a sample to the apparent rate at which CO₂ was diffused into the ICPEC. Those PECs prepared using only equal parts polyanion to polycation, both of a 50 mM concentration, showed two distinct regions of morphology visualized in Figure 3.13.

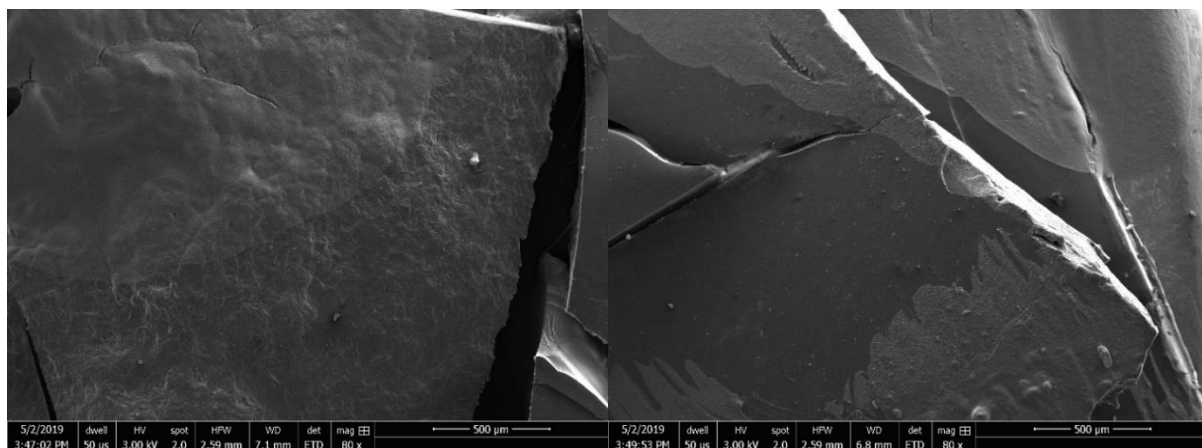


Figure 3.13 Images of the rough (left) and smooth (right) regions on a PEC under SEM at 80x magnification

Those regions formed on the portion of the PEC which was exposed to the atmosphere upon drying, inherited a morphology which is assumed to be indicative of surface regions where hydrophobic interactions dominate. Hydrophilic polyelectrolytes which are strongly associated with extrinsic local regions of high counterion concentration within are likely to migrate to the outer region of the PEC or ICPEC. Within these regions, little interpenetration of the polyelectrolytes occurs causing an apparent swelling of the complex which is thought to be associated with the rough morphology observed on the atmospheric drying fronts. This explanation is borrowed from effects which occur within polyelectrolyte multilayers which are consistent with those observed in the ICPECs.²⁰ These rough regions are where more non-systematic packing of the polyelectrolyte layers yield topographical formations which are very porous in nature.

Porosity on this scale and distribution as visualized in Figure 3.14 allows for diffusion of CO_2 into the ICPEC and formation of H_2CO_3 at a rate which would likely be unachievable in more ordered structures such as polyelectrolyte multilayers. Porosity on this scale however might also be indicative of vacancies left behind in the ICPEC structure as moisture rapidly evacuated

the surface layers when high vacuum is pulled on the ICPEC sample, as is necessary for analysis via SEM.

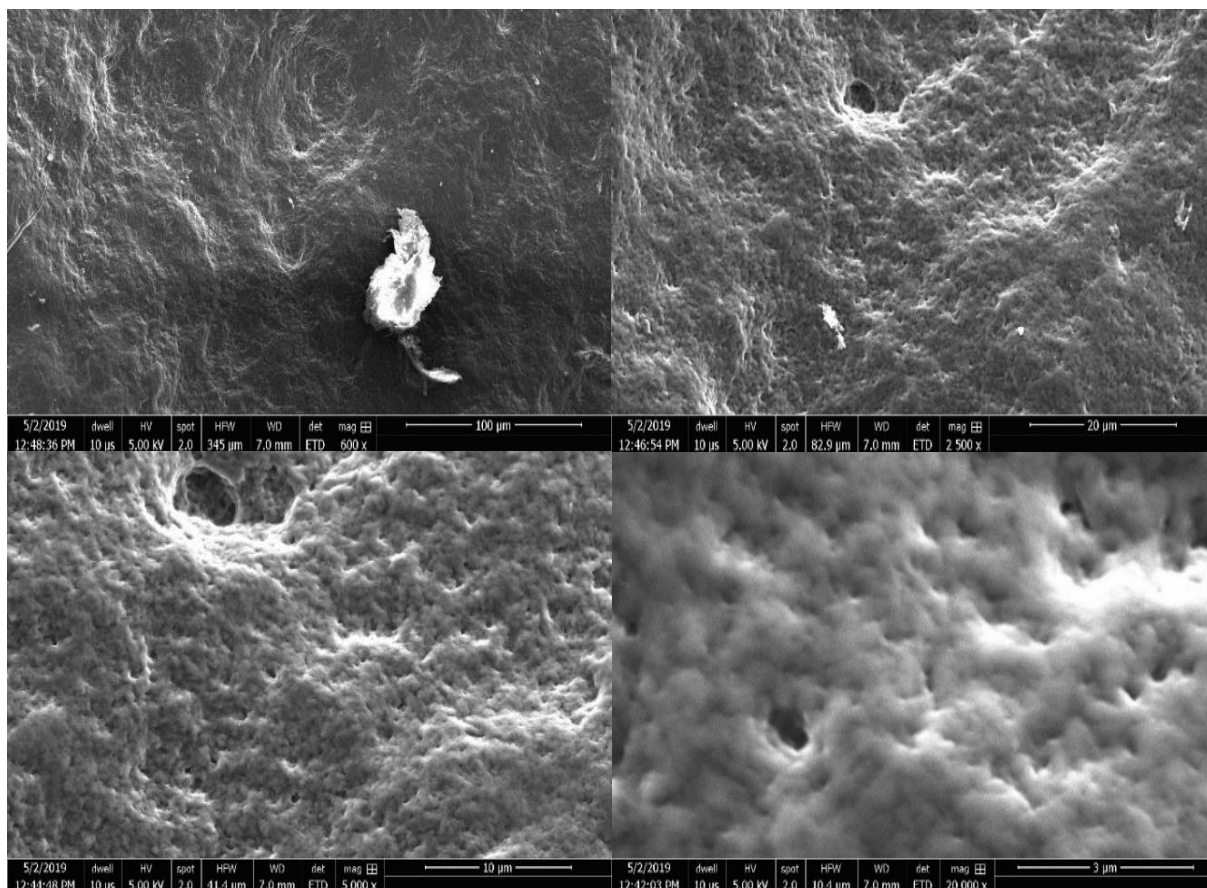


Figure 3.14 SEM images of the PEC rough structure at 600, 2500, 5000, and 20000x magnification.

Regions of the PEC or ICPEC which during drying were in contact with the glass slide appeared smooth and without much topological morphology. Formation of these smooth surfaces is not completely understood though it is suspected that during all phases of the preparation of the ICPEC the lower most layer maintains the least interaction with the solution phase of the complex mixture. This results in a layer in which the most hydrophobic and closely packed intrinsic polyelectrolyte interactions are occurring, yielding a smooth homogeneous surface

which more easily takes on the conformation of the substrate on which it is dried. Thorough mixing of the ICPEC post-precipitation could be seen to verify this explanation, as the ICPEC no longer forms a smooth region with the same degree of uniformity which is observed in the undisturbed ICPECs. Within the regions of the PEC or ICPEC in which these hydrophobic interactions dominate, close packing of the polyelectrolytes yields a more layer-by-layer structure in which very little porosity is observed as is visualized in Figure 3.15.

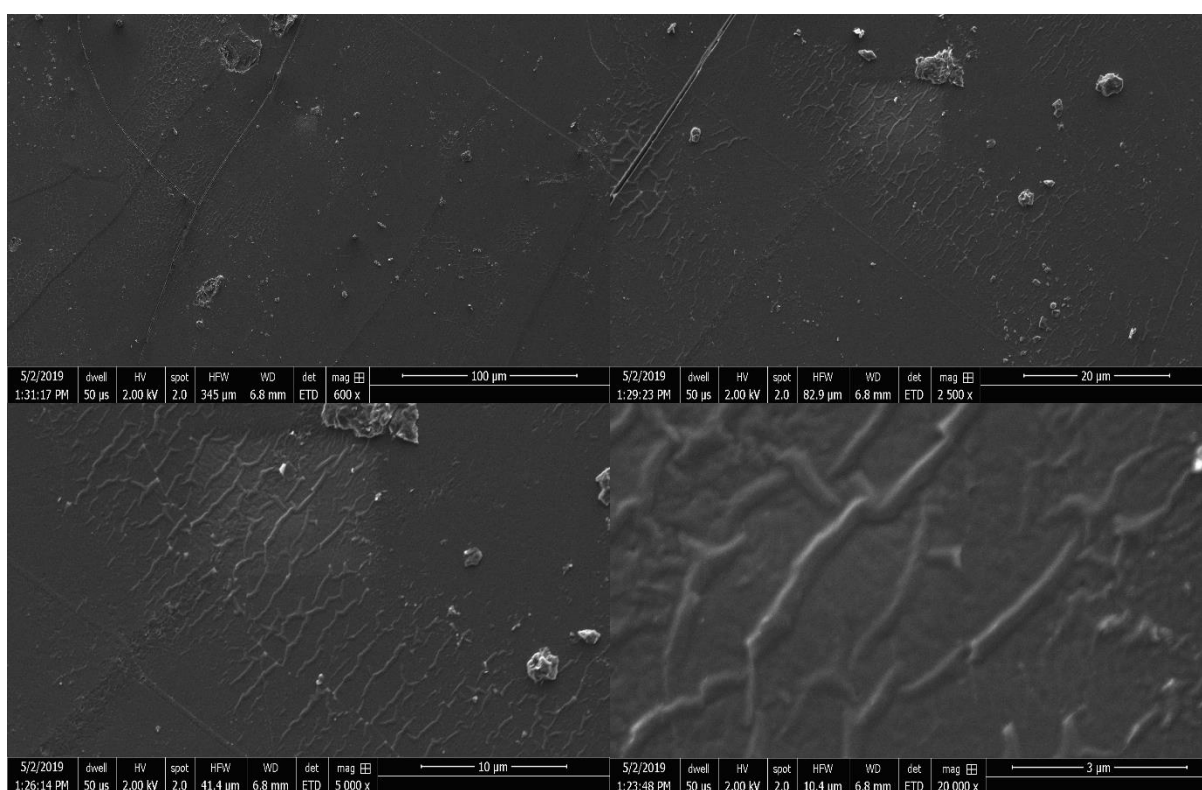


Figure 3.15 SEM images of the PEC smooth structure at 600, 2500, 5000, and 20000x magnification.

Preparation from the standard complex mixture yields ICPECs which are overall smooth in appearance, malleable, and maintain consistent dimensions with predictable distortion after drying. Visually it is apparent immediately upon precipitation of the ICPEC, that those complexes which are formed in variant reaction conditions have significantly modified

morphological properties. Most notably, those ICPECs which were prepared via complex mixtures with larger counterion concentrations showed considerable disruption in the surface topography when compared to those made under standard conditions.

Samples prepared with high counterion concentrations in the initial complex mixture also show expansion in volume from those dimensions imposed by the washer used for shaping the pellets before drying. As the samples expand in overall volume the pellets are observed to contract about the pellet perimeter and swell in height. This is consistent with migration of the counterions present within the ICPEC to the surface regions where hydrophilic counterion-polyelectrolyte interactions are favored, decreasing the interpenetration of polyelectrolytes, and therefore the density of those regions. This effect is compounded by the hydration spheres which accompany these counterions, further increasing the swelling. Contraction and accompanying surface deformity as observed in Figure 3.16 is observed in all samples with increased counterion concentration in the complex mixture.

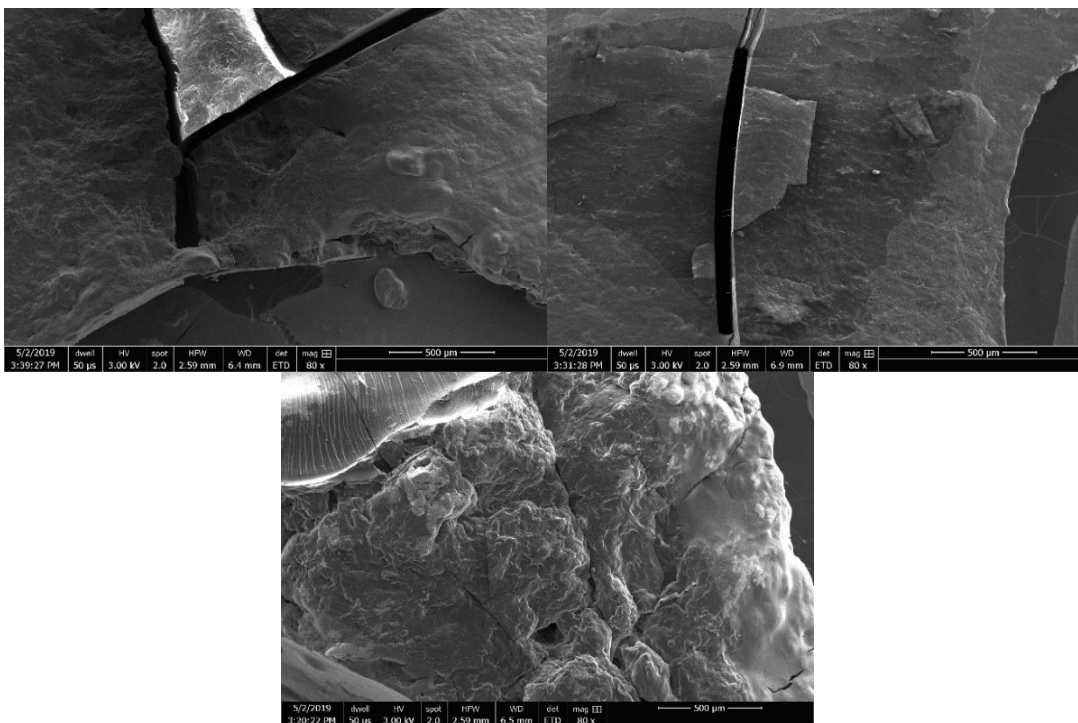


Figure 3.16 SEM images of PECs made under standard conditions (top left), with 50 mM NaCl (top right), and 250 mM NaCl (bottom)

Though surface deformity is evident in ICPECs prepared in solutions with increased counterion concentration, this disruption does not correlate with increased porosity within the ICPEC. As is seen in Figure 3.17 the porosity of the ICPEC surface is observed to decrease significantly on the micrometer scale as the concentration of counterion is increased. Smoothing of the ICPEC surface would likely occur during the swelling due to the same counterion migration and polyelectrolyte disruption mechanism previously described.

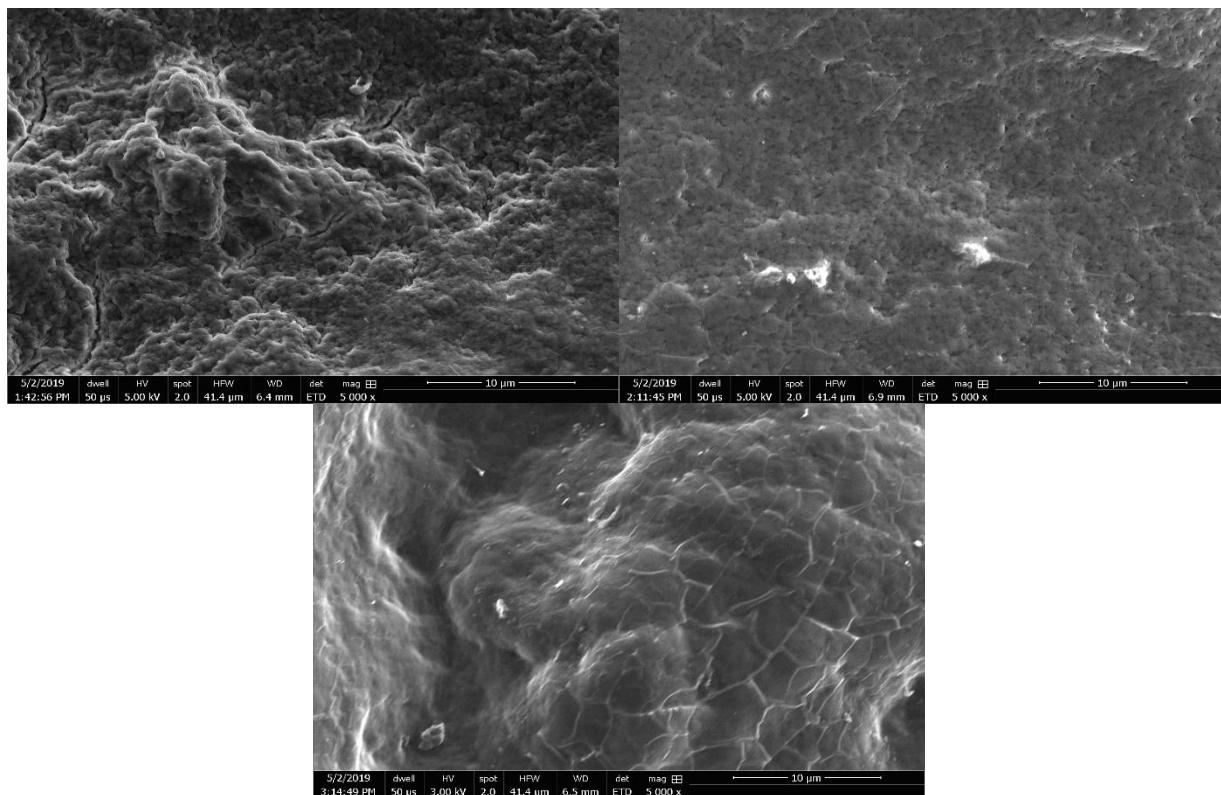


Figure 3.17 SEM images of PECs made under standard conditions (top left), with 50 mM NaCl (top right), and 250 mM NaCl (bottom) with an apparent trend of decreasing porosity as a function of counterion concentration

Resulting increases in the time response of the ICPECs are observed due to this decreased porosity present in high counterion concentration ICPECs. This time response is seen to positively correlate to the concentration of these counterions. Difficulties in determination of time response endpoints due to significant differences in ICPEC dried structures hinder the establishment of a more quantified correlation.

IV. Analysis of Polyelectrolyte Concentration

An eight-point standard curve was established for determination of PSSNa concentration present within the supernatant in terms of monomer units at the λ_{\max} of 224 nm yielding the equation seen in Figure 3.18. This value agrees well with literature values corresponding to the

max absorbing wavelength of PSSNa.³⁸ Utilizing the method established by Ziolkowska et al. a standard curve was established for PDADMAC-Bradford complex at the λ_{max} of 590 nm with a polynomial curve seen in Figure 3.19. Regardless of the standard calibration scale and sample gradient a polynomial curve was always observed as best-fit, even in seemingly more linear portions of the standard curve. Polynomial fit however yields calibration curves in which decreased response to concentration is observed in the spectral data as the concentration of the analyte increases. To mitigate this source of error only the lower 70% of any one PDADMAC-Bradford standard calibration range was utilized for the purpose of PDADMAC quantitation. Absorbances which corresponded to concentrations outside of this range on any one standard calibration were fit to a new calibration.

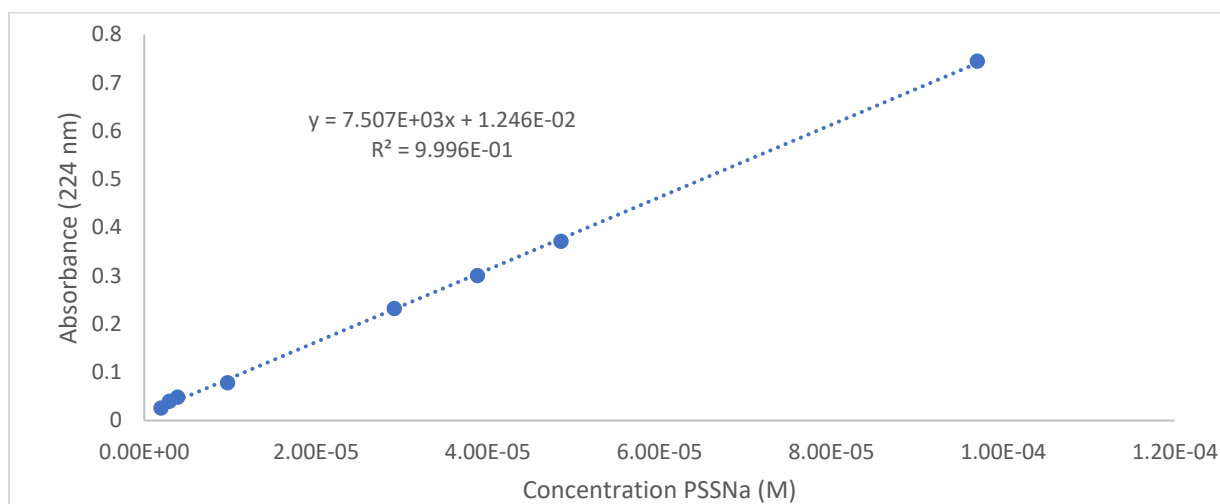


Figure 3.18 Linear calibration curve for PSSNa at 224 nm

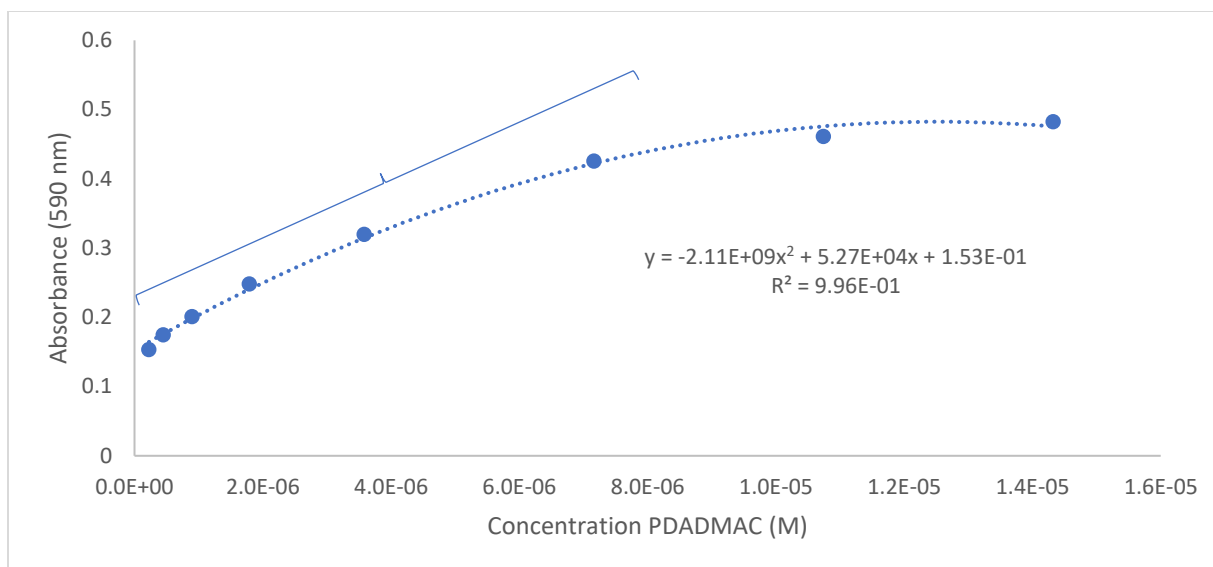


Figure 3.19 Standard calibration curve for PDADMAC at 590 nm. The bracketed region represents the approximate utilized region from 4.48×10^{-7} to 9.87×10^{-6}

It is known that the Bradford reagent binds to amine groups present within proteins during traditional use as a protein assay. It has been previously observed that this binding between the Coomassie Brilliant Blue 250-G present within the Bradford reagent and the amine groups in the analyte varies in intensity as a function of pH, Bradford reagent concentration, and analyte concentration.³⁴ While non-linear standard curves resulting from these effects do not adhere to Beer-Lambert's law, a correlation between sample concentration and absorbance at a single wavelength is still established assuming no change in pH and Bradford reagent concentration. Standards made for the calibration curve all maintained the same concentration of Bradford reagent.

Though the exact composition of the used Bradford reagent could not be obtained from Sigma, it is assumed to have a compositional similar to a traditional Bradford reagent mixture. If this is the case, the concentrated phosphoric acid which traditionally composes ~10% of the Bradford mixture will buffer the system with more than sufficient capacity to limit significant

change in pH within the calibration mixture as a function of varying analyte concentration. This assumption is perceived to hold true over close to three orders of magnitude as is observed in the standard calibration curve seen in Figure 3.19. It is noted that several absorbing wavelengths are present in the PDADMAC-Bradford complex absorption spectrum, each of which would require a separate calibration curve for a range of analyte concentrations as is seen in Figure 3.20.

The absorbing wavelength of 590 nm selected for the purpose of this research showed excellent concentration-absorbance correlation within the calibration concentration range, though selection of a different absorbing wavelength may have optimized the calibration curve over a larger concentration gradient. This max absorbing wavelength at 590 nm does differ from those selected within the literature. This discrepancy was determined to be derived largely from the aforementioned variation due to pH and analyte concentration.

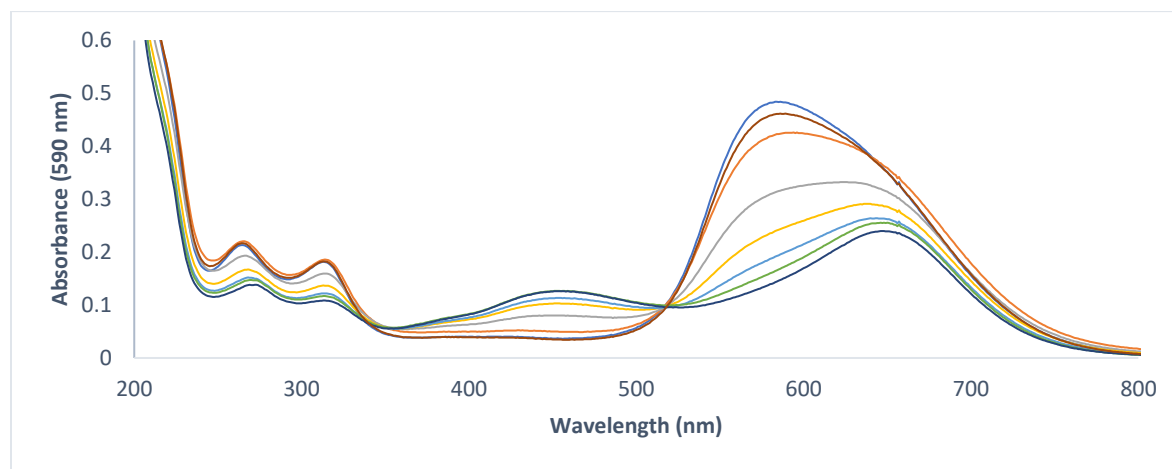
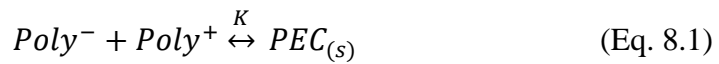


Figure 3.20 Stacked spectrum of the absorbance of PDADMAC as a function of increased concentration. Note the shift of the max absorbing wavelength on the peak ~ 590 nm.

Utilizing the standard curves for PSSNa and PDADMAC the concentrations of the supernatant solutions in each of the various dilutions was determined and used to find the final concentration of each of the polyelectrolytes within the supernatant solution. From these

polyelectrolyte concentrations it was possible to determine an equilibrium constant for the complexation of PDADMAC and PSSNa within these standard PEC formation conditions. From these concentrations it was possible to estimate the equilibrium constant of the PEC and ICPEC and therefore the Gibb's free energy associated with the complexation.

Polyelectrolyte complexation has been traditionally described as the titration of a polyanion with a polycation in a 1:1 ratio described by Equation 8.1. It should be noted that this equation is simplified when compared to the complete PEC complexation equation described in Equation 1.1 where counterions of each polyelectrolyte are accounted for. Within an ideal PEC the polycation and polyanion come together in a 1:1 ratio, expelling all counterions from extrinsic sites making only intrinsic polyelectrolyte pairs. With this ideal complexation assumption, the activities of the counterions are ignored as is seen in Equation 8.1. A simple equilibrium constant describing the formation of the PEC from the polyanion and polycation utilizing the known concentrations of polyanion and polycation remaining in solution can be then written as seen in Equation 8.2.



$$K \cong \frac{1}{[Poly^{-}][Poly^{+}]} \quad (\text{Eq. 8.2})$$

It is understood that in concentrated salt solutions this assumption will not hold true as has been seen extensively in other work.^{18,19} However, within dilute solutions, like those prepared in the standard method, the interaction of the counterions on the PEC or ICPEC complexation has been observed to be negligible, and those interactions have been ignored within this equilibrium.^{20,32}

$$\Delta G_{rxn}^{\circ} = -RT \ln K_{eq} \quad (\text{Eq. 8.3})$$

Values were calculated for the equilibrium constant K_{eq} and from those values the ΔG_{rxn}° for each of the two samples which represent PECs made under standard conditions using Gibb's equation (Eq. 8.3). In Table 3.11 the average change in Gibb's free energy for the formation of the standard PEC from PDADMAC and PSSNa was determined to be -29.7 kJ/mol assuming 20 °C laboratory conditions. This is consistent with the observed rapid formation of the PEC in laboratory conditions.

Table 3.10 Two standard PECs and the resulting concentrations of polycation and polyanion remaining in the supernatant solutions after precipitation of the PEC.

Sample ID	PSSNa Super. Conc. (mM)	PDADMAC Super. Conc. (mM)	ICPEC mol Ratio
PEC 3	1.81	2.19	1.008
95B	2.52	2.50	1.000

Table 3.11 Calculated values for K_{eq} and ΔG_{rxn}° of standard PECs assuming 20 °C as the laboratory temperature.

Sample ID	PSSNa Super. Conc. (mM)	PDADMAC Super. Conc. (mM)	$K_{eq}/10^5$	ΔG_{rxn}° (kJ/mol)
PEC 3	1.81	2.19	2.52	-30.3
95B	2.52	2.50	1.58	-29.2

Determination of the polyanion/polycation complexation ratios in ICPECs made using the standard method was carried out in the same manner using the polyelectrolyte concentrations seen in Table 3.12. It was found that the polyanion/polycation ratio within standard ICPECs was 0.977 ± 0.008 ($n = 9$). The Gibb's free energy of the ICPEC formation was determined to be -30.4 kJ/mol assuming 20 °C laboratory conditions as seen in Table 3.13.

Table 3.12 Concentrations and resulting mol ratios of the polyelectrolytes present in the supernatant solution after formation of the ICPEC made using the standard preparation method.

Sample ID	PSSNa Super. Conc. (mM)	PDADMAC Super. Conc. (mM)	ICPEC mol Ratio
94P 1	3.02	1.53	0.969
94P 2	3.04	1.31	0.964
94P 3	2.44	1.06	0.972
94P 4	2.16	1.38	0.984
94P 5	2.39	1.18	0.975
97PB 1	2.56	2.01	0.989
97PB 2	2.85	1.79	0.978
97PB 3	2.39	1.48	0.981
97PB 4	2.45	1.56	0.982

Table 3.13 Calculated values for K_{eq} and ΔG°_{rxn} of standard ICPECs assuming 20 °C as the laboratory temperature.

Sample ID	PSSNa Super. Conc. (mM)	PDADMAC Super. Conc. (mM)	$K_{eq}/10^5$	ΔG°_{rxn} (kJ/mol)
94P 1	3.02	1.53	2.17	-29.9
94P 2	3.04	1.31	2.51	-30.3
94P 3	2.44	1.06	3.87	-31.4
94P 4	2.16	1.38	3.34	-31.0
94P 5	2.39	1.18	3.53	-31.1
97PB 1	2.56	2.01	1.95	-29.7
97PB 2	2.85	1.79	1.96	-29.7
97PB 3	2.39	1.48	2.81	-30.6
97PB 4	2.45	1.56	2.63	-30.4

The lower average polyanion/polycation ratio observed in the standard ICPECs relative to the standard PECs is thought to be indicative of an increased presence of extrinsic pairs within the ICPEC which are not present within the PEC. Anionic association of the species produced by the boric acid buffer as well as the anionic pH indicator to the polycation present within the ICPECs complex mixture would interfere with the complexation of the ICPEC upon addition of the polyanion to solution.

As both the anionic species produced by the boric acid buffer and the pH sensitive indicator are significantly larger in ionic radius than the chloride anion which would be substituted, the

extrinsic pair size would be expected to have a corresponding increase in radius.³² Coupled with this factor, is the more reduced oxidation state of the pH sensitive indicator phenol red relative to the competing polyanion when present in solution at high pH, as well as the reduced oxidation state of the tetraborate species relative to the polyanion which is present in solution at high pH. While no direct study of the anionic species presented in this research in terms of polyelectrolyte complexation are known in previous literature, preferential anionic uptake by PECs with trends that relate roughly to those proposed have been extensively studied by other groups.³⁹

Comparing $\Delta G_{\text{rxn}}^{\circ}$ values of -29.7 and -30.4 kJ/mol for the standard PECs and ICPECs respectively implies the formation of the ICPEC product is not significantly hindered by the increased interaction of the ionic species present within the ICPEC complex mixture at those concentrations utilized. While it is known that the participation of these ionic species will certainly contribute to the equilibrium by which the complex is formed from the complex mixture to some degree, classification of these interactions exists in literature only in solutions with concentrations of ionic species, and therefore ionic activities, several orders of magnitude greater than those investigated during this research.^{17,19,32,35,36,40}

4. CONCLUSIONS

The ICPEC system has been characterized in order to determine potential utility as a medium in which pH sensitive indicators could be encapsulated for use as CO₂ sensitive device within environments such as medical device packaging. Investigation of the ICPEC system was performed: using various compositional modifications, while examining the rate at which the modified ICPEC reacts to introduction to CO₂; using UV-Vis analysis to determine the composition of the ICPEC, as well as the equilibrium by which formation of the ICPEC occurs; using STA analysis to determine the correlation between the internal moisture content of the ICPEC and the relative humidity of the environment in which it was formed; and using scanning electron microscopy to determine the morphological effects of increasing counterion concentration within the complex mixture.

Analysis of the internal moisture content of the standard PECs and ICPECs via STA determined internal moisture content under laboratory conditions to be 10 ± 2 and $12 \pm 3\%$ by mass respectively. Equilibrium with atmospheric humidity was found to be rapidly established in as little as 24 hours in both cases and is believed to be accelerated by migration of the internal water content within these materials to surface regions where evaporation can occur. Migration of internal moisture to the surface is thought to be promoted by entropic driving forces which prefer intrinsic polyanion/polycation pairing to extrinsic polyelectrolyte/counterion pairing. This leads to segregation of ionic hydration spheres against the surface where moisture can be removed via evaporation, further reducing extrinsic pairing within the ICPEC via interpenetration of polyelectrolytes for additional charge compensation. Confirmation of this internal moisture migration to surface regions was observed via ATIR-FTIR through increased IR absorbance correlating to the stretching modes of water at 3400 cm^{-1} over the course of three

days. That is, it was observed that there was an increased presence of water at the surface of the ICPEC, via ATR-FTIR, with simultaneous decrease in total ICPEC water content, determined via STA.

Evaluation via time lapse photography revealed ICPECs which were dried at an increased temperature of 70 °C for one hour prior to standard equilibration at room temperature showed decreased sensitivity to introduction of high concentrations of CO₂ as well as near complete loss of reversible color change. Samples treated in this way underwent color change 50–750% slower upon introduction to high concentrations of atmospheric CO₂ relative to those samples prepared using the standard method. Significantly increased transition time of the encapsulated indicator is attributed largely to the rapid loss of internal moisture within the ICPEC surface regions, which accounts for a large fraction of the ICPEC total internal moisture due to migration of water to the surface region of the ICPEC. This decreased internal water content within the ICPEC increases the effective internal buffer capacity and therefore increases the quantity of diffused CO₂ which must be present in order to produce acidic conditions which yield colorimetric transitions from the encapsulated indicator as it becomes protonated.

Time lapse photography of the salted ICPECs in which higher concentrations of counterions were present in the complex mixtures revealed increased time response to introduction to high concentrations of CO₂. Final time responses of ICPECs formed in complex mixtures with counterionic concentrations of 50 mM were observed to increase ~200% relative to ICPECs formed using the standard method. Solutions containing counterionic concentrations of 250 mM were observed to have increased time responses ranging from 300–500% that of ICPECs prepared using the standard method. Increased time response was largely attributed to ionic swelling within the ICPEC though paired with information gained from SEM analysis of the

salted samples it was concluded that increased time response is likely due to decreased surface porosity which limits diffusion of CO₂ into the ICPEC.

Time lapse photography allowed also for a correlation between effective buffer capacity of an ICPEC system and time response to introduction of high atmospheric CO₂ concentrations to be established. It was concluded that the protonation rate of the encapsulated pH sensitive indicator was reduced due to the significantly increased buffer capacity present within an ICPEC which were in turn due to polyelectrolyte concentration as well as preferential pairing of ionic buffering species to extrinsic sites within the ICPEC.

Finally, time lapse photography of the introduction of ICPECs to high concentration CO₂ environments determined ICPECs which were exposed to environments with high relative humidities responded more rapidly than those prepared under standard conditions. Decreased time response in these samples is attributed to the same correlation between internal moisture content of the ICPEC and internal buffer capacity that was established in the examination of samples which were dried at higher temperatures. That is, ICPECs which contain a larger degree of internal moisture have decreased activity of the ionic buffering species present due to dilution of the buffering species within the ICPEC. In turn this leads to decreased time response in those samples which have come to equilibrium with atmospheres with higher concentrations of water vapor present. It is speculated that significantly decreased water content within the ICPEC could limit the mobility of dissolved CO₂ within the system, therefore limiting the amount of pH sensitive indicator which can be acidified, decreasing the observed time response upon introduction to CO₂.

Analysis of the polyelectrolyte concentrations within the supernatant solution following precipitation of both PECs and ICPECs was accomplished via UV-Vis spectroscopy and

utilization of the PSSNa polyanion absorption at 224 nm and the PDADMAC-Bradford complex absorption at 590 nm. These supernatant polyelectrolyte concentrations when subtracted from the known initial polyelectrolyte concentrations allowed for determination of the ratio of polyelectrolyte association within the PEC or ICPEC. These values were determined to be 1.004 ± 0.006 and 0.977 ± 0.008 for the formation of PECs and ICPECs respectively. Estimates of the K_{eq} and therefore the ΔG°_{rxn} for both PECs and ICPECs were also possible utilizing the supernatant polyelectrolyte concentrations. Average estimated free energy for the formation of PECs from PDADMAC and PSSNa from initial 50 mM concentrations was calculated to be - 29.7 kJ/mol. Average estimated free energy for the formation of ICPECs from PDADMAC and PSSNa from initial 50 mM concentrations in the standard complex mixture was calculated to be - 30.4 kJ/mol. These values indicate the additional ionic strength contribution from the boric acid buffer and the phenol red species present within the standard ICPEC complex mixture does not significantly reduce the formation of the ICPEC relative to the formation of standard PECs.

The indicator containing polyelectrolyte complex is a novel method by which detection of atmospheric carbon dioxide can be accomplished. Materials for formation of these complexes can be obtained cheaply and complexes can be formed reproducibly in a rapid one-step process. These materials have shown to be very sensitive to internal humidity and ionic concentration and therefore can be easily tuned for specific time responses upon introduction to high concentrations of atmospheric carbon dioxide. Research summarized by this thesis presents methods by which control over those tuning parameters can be achieved, as well as properties which could be further investigated to expand understanding of these intricate systems. Potential use of indicator containing polyelectrolyte complexes within various industrial applications is considerable and further investigation of these systems should be pursued.

5. References

- (1) Mills, A.; Chang, Q.; McMurray, N. Equilibrium Studies on Colorimetric Plastic Film Sensors for Carbon Dioxide. *Anal. Chem.* **1992**, *64* (13), 1383–1389.
<https://doi.org/10.1021/ac00037a015>.
- (2) Heacock, G.; Rivera, D. Color Changeable Dyes for Indicating Exposure, Methods of Making and Using Such Dyes, and Apparatuses Incorporating Such Dyes. 8663998, 2014.
<https://doi.org/10.1145/634067.634234>.
- (3) Byrne, R. H. Measuring Ocean Acidification: New Technology for a New Era of Ocean Chemistry. *Environ. Sci. Technol.* **2014**, *48* (10), 5352–5360.
<https://doi.org/10.1021/es405819p>.
- (4) Daniels, J. A.; Krishnamurthi, R.; Rizvi, S. S. H. A Review of Effects of Carbon Dioxide on Microbial Growth and Food Quality. *J. Food Prot.* **1985**, *48* (6), 532–537.
<https://doi.org/10.4315/0362-028X-48.6.532>.
- (5) Theodore P Labuza, W. B. Application of ‘Active Packaging’ Technologies for the Improvement of Shelf-Life and Nutritional Quality of Fresh and Extended Shelf-Life Foods. *J. Food Process. Preserv.* **1989**, *43*, 1–69.
- (6) Biji, K. B.; Ravishankar, C. N.; Mohan, C. O.; Srinivasa Gopal, T. K. Smart Packaging Systems for Food Applications: A Review. *J. Food Sci. Technol.* **2015**, *52* (10), 6125–6135. <https://doi.org/10.1007/s13197-015-1766-7>.
- (7) Fuente, J. de la; Bix, L. *Medical Device Packaging*; 2009.
<https://doi.org/10.13140/RG.2.1.1717.2964>.
- (8) Zeman, S.; Kubík, L. Permeability of Polymeric Packaging Materials. *Tech. Sci.* **2007**, *10*, 33–34. <https://doi.org/10.2478/v10022-007-0004-6>.

- (9) Mills, A.; Tommons, C.; Bailey, R. T.; Tedford, M. C.; Crilly, P. J. UV-Activated Luminescence/Colourimetric O₂ Indicator. *Int. J. Photoenergy* **2008**, 2008, 1–6.
<https://doi.org/10.1155/2008/547301>.
- (10) Von Bültzingslöwen, C.; McEvoy, A. K.; McDonagh, C.; MacCraith, B. D.; Klimant, I.; Krause, C.; Wolfbeis, O. S. Sol–Gel Based Optical Carbon Dioxide Sensor Employing Dual Luminophore Referencing for Application in Food Packaging Technology. *Analyst* **2002**, 127 (11), 1478–1483. <https://doi.org/10.1039/B207438A>.
- (11) Mills, A.; Tommons, C.; Bailey, R. T.; Tedford, M. C.; Crilly, P. J. UV-Activated Luminescence/Colourimetric O₂ Indicator. *Int. J. Photoenergy* **2008**, 2008, 1–6.
<https://doi.org/10.1155/2008/547301>.
- (12) Lee, S.; Sheridan, M.; Mills, A. Novel UV-Activated Colorimetric Oxygen Indicator. *Chem. Mater.* **2005**, 17 (10), 2744–2751. <https://doi.org/10.1021/cm0403863>.
- (13) Mills, A.; McMurray, H. Carbon Dioxide Monitor. WO 91/05252, 1991.
- (14) Heacock, G. Apparatuses, Indicators, Methods and Kits with Timed Color Change Indication. 9746421, 2017.
- (15) Rickard, C. M.; McCann, D.; Munnings, J.; McGrail, M. R. Routine Resite of Peripheral Intravenous Devices Every 3 Days Did Not Reduce Complications Compared with Clinically Indicated Resite: A Randomised Controlled Trial. *BMC Med.* **2010**, 8 (1), 53.
<https://doi.org/10.1186/1741-7015-8-53>.
- (16) Acar, N.; Huglin, M. B.; Tulun, T. Complex Formation between Poly(Sodium Phosphate) and Poly(4-Vinylpyridinium Chloride) in Aqueous Solution. *Polymer (Guildf)*. **1999**, 40 (23), 6429–6435. [https://doi.org/10.1016/S0032-3861\(99\)00060-9](https://doi.org/10.1016/S0032-3861(99)00060-9).
- (17) Fares, H. M.; Schlenoff, J. B. Equilibrium Overcompensation in Polyelectrolyte

- Complexes. *Macromolecules* **2017**, *50* (10), 3968–3978.
<https://doi.org/10.1021/acs.macromol.7b00665>.
- (18) Kaiser, C. The Characterization of Coacervate Systems Using Redox Sensative Dyes. **2018**, 1–127.
- (19) Wang, Q.; Schlenoff, J. B. The Polyelectrolyte Complex/Coacervate Continuum. *Macromolecules* **2014**, *47* (9), 3108–3116. <https://doi.org/10.1021/ma500500q>.
- (20) Dubas, S. T.; Schlenoff, J. B. Factors Controlling the Growth of Polyelectrolyte Multilayers. *Macromolecules* **1999**, *32* (24), 8153–8160.
<https://doi.org/10.1021/ma981927a>.
- (21) Hoene, B.; Rivera, D. Optical Studies of the Solution Phase Reduction and Stabilization of Indigo Tetrasulfonate in Polyelectrolyte Complexes. *Heliyon* **2017**, *3* (9), e00397.
<https://doi.org/10.1016/j.heliyon.2017.e00397>.
- (22) Hoene, B. Kinetic Decay of a Polymer/Ink Complex as an O₂ Indicator, Central Washington University, WA, 2016.
- (23) Mueller, R.; Köhler, K.; Weinkamer, R.; Sukhorukov, G.; Fery, A. Melting of PDADMAC/PSS Capsules Investigated with AFM Force Spectroscopy. *Macromolecules* **2005**, *38* (23), 9766–9771. <https://doi.org/10.1021/ma0513057>.
- (24) Köhler, K.; Shchukin, D. G.; Sukhorukov, G. B.; Möhwald, H. Drastic Morphological Modification of Polyelectrolyte Microcapsules Induced by High Temperature. *Macromolecules* **2004**, *37* (25), 9546–9550. <https://doi.org/10.1021/ma048474w>.
- (25) Köhler, K.; Shchukin, D. G.; Möhwald, H.; Sukhorukov, G. B. Thermal Behavior of Polyelectrolyte Multilayer Microcapsules. 1. The Effect of Odd and Even Layer Number. *J. Phys. Chem. B* **2005**, *109* (39), 18250–18259. <https://doi.org/10.1021/jp052208i>.

- (26) Köhler, K.; Möhwald, H.; Sukhorukov, G. B. Thermal Behavior of Polyelectrolyte Multilayer Microcapsules: 2. Insight into Molecular Mechanisms for the PDADMAC/PSS System. *J. Phys. Chem. B* **2006**, *110* (47), 24002–24010.
<https://doi.org/10.1021/jp062907a>.
- (27) Fu, J.; Wang, Q.; Schlenoff, J. B. Extruded Superparamagnetic Saloplastic Polyelectrolyte Nanocomposites. *ACS Appl. Mater. Interfaces* **2015**, *7* (1), 895–901.
<https://doi.org/10.1021/am5074694>.
- (28) Farhat, T.; Yassin, G.; Dubas, S. T.; Schlenoff, J. B. Water and Ion Pairing in Polyelectrolyte Multilayers. *Langmuir* **1999**, *15* (20), 6621–6623.
<https://doi.org/10.1021/la990631a>.
- (29) Leporatti, S.; Gao, C.; Voigt, A.; Donath, E.; Möhwald, H. Shrinking of Ultrathin Polyelectrolyte Multilayer Capsules upon Annealing: A Confocal Laser Scanning Microscopy and Scanning Force Microscopy Study. *Eur. Phys. J. E* **2001**, *5* (1), 13–20.
<https://doi.org/10.1007/s101890170082>.
- (30) Kristen, N.; Vüllings, A.; Laschewsky, A.; Miller, R.; von Klitzing, R. Foam Films from Oppositely Charged Polyelectrolyte/Surfactant Mixtures: Effect of Polyelectrolyte and Surfactant Hydrophobicity on Film Stability. *Langmuir* **2010**, *26* (12), 9321–9327.
<https://doi.org/10.1021/la1002463>.
- (31) Jaber, J. A.; Schlenoff, J. B. Counterfoils and Water in Polyelectrolyte Multilayers: A Tale of Two Polycations. *Langmuir* **2007**, *23* (2), 896–901. <https://doi.org/10.1021/la061839g>.
- (32) Fu, J.; Fares, H. M.; Schlenoff, J. B. Ion-Pairing Strength in Polyelectrolyte Complexes. *Macromolecules* **2017**, *50* (3), 1066–1074.
<https://doi.org/10.1021/acs.macromol.6b02445>.

- (33) Greenspan, L. Humidity Fixed Points of Binary Saturated Aqueous Solutions. *J. Res. Natl. Bur. Stand. Sect. A Phys. Chem.* **1977**, *81A* (1), 89. <https://doi.org/10.6028/jres.081A.011>.
- (34) Ziolkowska Dorota; Shyichuk, A.; Zelazko, K. A New Method of Spectrophotometric Determination of Poly(Diallyldimethylammonium Chloride) Concentration. *Polimery* **2012**, *57* (4), 303–305. <https://doi.org/10.14314/polimery.2012.303>.
- (35) Fares, H. M.; Wang, Q.; Yang, M.; Schlenoff, J. B. Swelling and Inflation in Polyelectrolyte Complexes. *Macromolecules* **2019**, *52* (2), 610–619. <https://doi.org/10.1021/acs.macromol.8b01838>.
- (36) Fares, H. M.; Schlenoff, J. B. Diffusion of Sites versus Polymers in Polyelectrolyte Complexes and Multilayers. *J. Am. Chem. Soc.* **2017**, *139* (41), 14656–14667. <https://doi.org/10.1021/jacs.7b07905>.
- (37) Yang, M.; Shi, J.; Schlenoff, J. B. Control of Dynamics in Polyelectrolyte Complexes by Temperature and Salt. *Macromolecules* **2019**, *52* (5), 1930–1941. <https://doi.org/10.1021/acs.macromol.8b02577>.
- (38) Su, N.; Li, H.; Huang, Y.; Zhang, X. Synthesis of Salt Responsive Spherical Polymer Brushes. *J. Nanomater.* **2015**, *2015*, 1–7. <https://doi.org/10.1155/2015/956819>.
- (39) Ghostine, R. A.; Shamoun, R. F.; Schlenoff, J. B. Doping and Diffusion in an Extruded Saloplastic Polyelectrolyte Complex. *Macromolecules* **2013**, *46* (10), 4089–4094. <https://doi.org/10.1021/ma4004083>.
- (40) Delgado, J. D.; Schlenoff, J. B. Static and Dynamic Solution Behavior of a Polyzwitterion Using a Hofmeister Salt Series. *Macromolecules* **2017**, *50* (11), 4454–4464. <https://doi.org/10.1021/acs.macromol.7b00525>.